25. Suwannasaen D, Romphruk A, Leelayuwat C, Lertmemongkolchai G (2010) Bystander T cells in human immune responses to dengue antigens. BMC Immunol 11:47
26. Vaughn DW, Green S, Kalayanarooj S, Innis BL, Nimmannitya S, Suntayakorn S, Endy TP, Raengsakulrach B, Rothman AL, Ennis FA, Nisalak A (2000) Dengue viremia titer, antibody response pattern, and virus serotype correlate with disease severity. J Infect Dis 181:2–9
27. Wahid SF, Sanusi S, Zawawi MM, Ali RA (2000) A comparison of the pattern of liver involvement in dengue hemorrhagic fever with classic dengue fever. Southeast Asian J Trop Med Public Health 31:259–263
28. Woollard DJ, Haqshenas G, Dong X, Pratt BF, Kent SJ, Gowans EJ (2008) Virus-specific T-cell immunity correlates with control of GB virus B infection in marmosets. J Virol 82:3054–3060
29. Yoshida T, Saito A, Iwasaki Y, Iijima S, Kurosawa T, Katakai Y, Yasutomi Y, Reimann KA, Hayakawa T, Akari H (2010) Characterization of natural Killer cells in tamarins: a technical basis for studies of innate immunity. Front Microbiol 1:128. doi: 10.3389/fmicb.2010.00128

ELSEVIER

INSTITUT PASTEUR

Microbes and Infection 13 (2011) 58–64

www.elsevier.com/locate/micinf

Original article

Improved capacity of a monkey-tropic HIV-1 derivative to replicate in cynomolgus monkeys with minimal modifications

Akatsuki Saito [a,b,c,1], Masako Nomaguchi [d,1], Sayuki Iijima [c], Ayumu Kuroishi [e], Tomoyuki Yoshida [b], Young-Jung Lee [c], Toshiyuki Hayakawa [b], Ken Kono [e], Emi E. Nakayama [e], Tatsuo Shioda [e], Yasuhiro Yasutomi [c], Akio Adachi [d], Tetsuro Matano [a], Hirofumi Akari [b,c,*]

[a] *International Research Center for Infectious Diseases, The Institute of Medical Science, The University of Tokyo, Tokyo 108-8639, Japan*
[b] *Primate Research Institute, Kyoto University, Inuyama 484-8506, Japan*
[c] *Tsukuba Primate Research Center, National Institute of Biomedical Innovation, Tsukuba 305-0843, Japan*
[d] *Department of Microbiology, Institute of Health Biosciences, The University of Tokushima Graduate School, Tokushima 770-8503, Japan*
[e] *Department of Viral Infections, Research Institute for Microbial Diseases, Osaka University, Suita 565-0871, Japan*

Received 31 July 2010; accepted 1 October 2010
Available online 16 October 2010

Abstract

Human immunodeficiency virus type 1 (HIV-1) hardly replicates in Old World monkeys. Recently, a mutant HIV-1 clone, NL-DT5R, in which a small part of *gag* and the entire *vif* gene are replaced with SIVmac239-derived ones, was shown to be able to replicate in pigtail monkeys but not in rhesus monkeys (RM). In the present study, we found that a modified monkey-tropic HIV-1 (HIV-1mt), MN4-5S, acquired the ability to replicate efficiently in cynomolgus monkeys as compared with the NL-DT5R, while neither NL-DT5R nor MN4-5S replicated in RM cells. These results suggest that multiple determinants may be involved in the restriction of HIV-1 replication in macaques, depending on the species of macaques. The new HIV-1mt clone will be useful for studying molecular mechanisms by which anti-viral host factors regulate HIV-1 replication in macaques.

Keywords: HIV-1; Old World monkey; TRIM5α

1. Introduction

Human immunodeficiency virus type 1 (HIV-1) productively infects only humans but not Old World monkeys (OWM) such as cynomolgus monkeys (CM) or rhesus monkeys (RM), whereas RM-derived simian immunodeficiency virus (SIVmac) can efficiently replicate in OWM. Because of this species barrier, alternative monkey models using SIVmac or simian/human immunodeficiency viruses (SHIV) have been used for AIDS research [1–4]. However, detailed analyses of molecular mechanisms of the pathogenesis of HIV-1 have been hampered by the lack of appropriate non-human primate models for HIV-1 infection.

The mechanistic basis for the inability of HIV-1 to replicate in OWM cells has remained unclear. Recently, a number of intrinsic anti-HIV-1 cellular factors, including tripartite motif protein 5α (TRIM5α), Cyclophilin A (CypA), apolipoprotein B mRNA-editing catalytic polypeptide (APOBEC3) family and Tetherin were discovered in OWM cells [5,6]. TRIM5α strongly suppresses HIV-1 replication, mainly by affecting the viral disassembly step, resulting in a decrease of reverse transcription products [7,8]. CypA acts as a regulator promoting TRIM5α-mediated restriction of HIV-1 [8]. APOBEC3 is also a major regulator of HIV-1 replication [9,10]. APOBEC3 exerts its inhibitory effect mainly by inducing G to A hypermutation

* Corresponding author. Primate Research Institute, Kyoto University, Inuyama 484-8506, Japan. Tel.: +81 568 63 0440; fax: +81 568 63 0459.
E-mail address: akari@pri.kyoto-u.ac.jp (H. Akari).
[1] A.S. and M.N. contributed equally to this work.

1286-4579/$ - see front matter © 2010 Institut Pasteur. Published by Elsevier Masson SAS. All rights reserved.
doi:10.1016/j.micinf.2010.10.001

into the viral genome due to its cytidine deaminase activity, while hypermutation-independent inhibitory activity at the stage of reverse transcription is also evident [11]. Tetherin, also referred to as a BST-2, was identified as an intrinsic anti-viral factor that restricts the egress of HIV-1 by tethering virions to the host cell surface [12,13]. Importantly, HIV-1 can counteract human APOBEC3 activity by utilizing the viral accessory protein Vif, whereas it cannot counteract OWM APOBEC3 [14]. Similarly, HIV-1 counteracts human Tetherin activity by utilizing another viral accessory protein Vpu, whereas HIV-1 does not counteract OWM Tetherin activity [15].

In an attempt to generate a monkey-tropic HIV-1 (HIV-1mt), Kamada et al. constructed an HIV-1 variant carrying minimal SIVmac-derived sequences to overcome the restriction factors [16]. The prototype HIV-1 clone NL-DT5R had a sequence encoding an SIVmac loop between alpha helices 4 and 5 (L4/5) of *capsid* gene (CA) and the entire *vif* gene, which relieved the inhibitory effects on viral replication by restriction factors CypA, TRIM5α and APOBEC3. NL-DT5R was able to replicate in pigtail monkeys (PM) in vivo as well as in vitro, as reported by Igarashi et al. [17]. Although NL-DT5R induced immune responses in infected animals, the virus did not establish persistent infection.

In the present study, we sought to adapt NL-DT5R to CM by performing long-term passage in CM-derived HSC-F cells. We successfully obtained a modified HIV-1mt clone having several mutations. Additionally, we inserted an SIVmac loop between alpha helices 6 and 7 (L6/7) of CA [18]. The resultant clone named MN4-5S was found to replicate efficiently and to induce strong immune responses in infected CM, suggesting the impact of viral adaptation.

2. Materials and methods

2.1. Plasmid construction

The HIV-1 derivatives were constructed on a background of an infectious molecular clone, NL4-3 [19]. NL-DT5R, a cloned virus containing SIVmac239 L4/5 and the entire *vif* gene, was reported previously by Kamada et al. [16]. In addition, NL-DT562, a virus having an R5-tropic SF162-derived *env* gene on a background of NL-DT5R, was used in this study [20]. After long passage of NL-DT5R and NL-DT562 in cynomolgus T cell line HSC-F [21], several mutations were appeared in both viral genomes, and then all of them were inserted into NL-DT5R by gene-engineering techniques. Consequently, a clone having 14 nucleotide substitutions in its genome was constructed and named MN4-5. Among these substitutions, 7 were non-synonymous mutations. The structure of the clone is shown in Fig. 1. A part of L6/7 of CA (aa residues 120–122; HNP) of MN4-5 was also replaced with the corresponding segment of SIVmac239 CA (aa residues 120–123; RQQN) by means of site-directed mutagenesis as described previously in Ref. [18]. The resultant construct was designated MN4-5S.

2.2. Cells and viruses

Human embryonic kidney cell line HEK293T was maintained in DMEM supplemented with 10% fetal bovine serum, 100 units/ml of penicillin and 100 μg/ml of streptomycin (Sigma). Monkey peripheral blood mononuclear cells (PBMCs) were separated with a standard Ficoll density gradient separation method and cultured in R-10 composed of

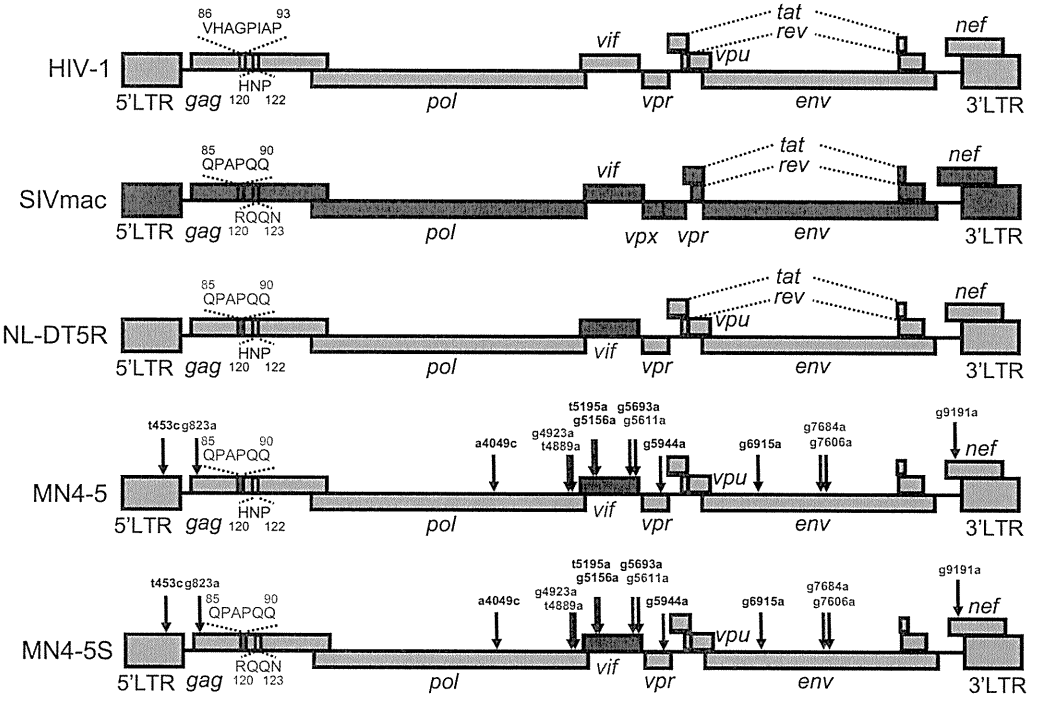

Fig. 1. Structure of HIV-1mt clones used in this study. The positions of nucleotide mutations are indicated by arrows in this figure. Among nucleotide substitutions, the positions of non-synonymous mutations are indicated in red.

RPMI-1640 medium supplemented with 10% fetal bovine serum, 100 units/ml of penicillin and 100 μg/ml of streptomycin (Sigma). The growth kinetics of each HIV-1 clone were examined in activated $CD8^+$ cell-depleted PBMCs. Briefly, separated PBMCs were reacted with a PE-labeled anti-CD8 antibody and then treated with anti-PE magnetic beads. After washing, $CD8^+$ cell-depleted PBMCs were negatively separated by using MACS columns (Miltenyi Biotec). For stimulation, $CD8^+$ cell-depleted PBMCs were first cultured in R-10 containing 1 μg/ml of concanavalin A (Sigma) for 2 days followed by culture in R-10 supplemented with 100 U/ml IL-2 (Shionogi) for more 2 days. The cells were then infected with 100 ng of p24 of HIV-1 and the culture supernatant was collected periodically. HSC-F, a cynomolgus monkey-derived $CD4^+$ T cell line [21], was cultured in R-10.

Virus stocks were prepared as follows: sub-confluent HEK293T cells were transfected with proviral DNA using Lipofectamine2000 reagent according to the manufacturer's instructions. At 42 h after transfection, culture supernatants were centrifuged, filtrated with a 0.45 μm filter, and aliquoted as virus stocks for in vitro experiments. For preparation of viral stocks for in vivo experiments, $CD8^+$ cell-depleted PBMCs were infected with the HEK293T-derived stocks as described above. After washing, the cells were maintained for several days and the culture supernatants were collected and stored as described above.

2.3. Reverse transcription (RT) assay

Virion-associated RT activity was measured as described previously in Ref. [22]. HSC-F cells (1×10^6) were infected with equal amounts of viruses (1×10^7 RT units). Viral growth kinetics was determined by RT production in the culture supernatants.

2.4. Animal experiments

Healthy adult cynomolgus monkeys were used in this study. All animals were confirmed to be negative for simian retrovirus and were housed in individual isolators in a biosafety level 3 facility and maintained according to the National Institute of Biomedical Innovation rules and guidelines for experimental animal welfare. Bleeding and viral inoculation were performed under ketamine hydrochloride anesthesia. Viral stocks for inoculation were inoculated into each animal. The profiles of plasma viral RNA loads, circulating $CD4^+$ and $CD8^+$ T lymphocytes were evaluated as described below.

2.5. Flow cytometry and immunophenotyping of peripheral blood lymphocytes

Immunophenotyping of freshly isolated PBMCs was performed according to standard procedures using multicolor flow cytometry performed with a FACSCantoII (Becton Dickinson). $CD4^+$ and $CD8^+$ T cells were identified using monoclonal antibodies (mAbs) to CD3 (clone SP34-2, BD Pharmingen), CD4 (clone L200, BD Pharmingen) and CD8 (clone DK25, DAKO). Flow cytometric acquisition and analysis of samples was performed on at least 10,000 events collected by a flow cytometer driven by FACSDiVa software.

2.6. Analysis of anti-viral antibody response

Plasma samples from infected animals were first heat-inactivated at 56 °C for 30 min. Then, 100-fold diluted samples were reacted with commercially available anti-HIV-1 antibody detection strips (New LAV Blot I, Bio-Rad) according to the manufacture's instructions.

2.7. In vivo depletion of $CD8^+$ lymphocytes

Infected animals received an anti-CD8 mAb (cM-T807) as follows: 10 mg/kg (body weight) inoculation subcutaneously at 42 days post infection (DPI), followed by 5 mg/kg inoculation intravenously at 45, 49, and 52 DPI. The cM-T807 mAb was provided by the NIH Nonhuman Primate Reagent Resource. To repeatedly confirm the depletion of $CD8^+$ cells in the presence of cM-T807, an anti-CD8 mAb (clone DK25, DAKO) was used as reported previously in Ref. [23].

2.8. Quantification of viral RNA

Total RNA was collected from monkey plasma using a High Pure Viral RNA Kit (Roche Diagnostics) according to the manufacturer's instructions. Viral RNA was quantified with a quantitative real-time PCR system using TaqMan One-Step RT-PCR Master Mix Reagents (Applied Biosystems). The primers and probe used in this study were as follows: Forward primer: HIVgag683 (+) (5′-CTCTCGACGCAGGACTCGGCTTGCT-3′); Reverse primer: HIVgag803 (−) (5′-GCTCTCGCACCCATCTCTCTCCTTCTAGCC-3′); Probe: HIVgag TaqMan 720R748 (FAM-GCAAGAGGCGAGRGGCGGCGACTGGTGAG-TAMRA). The quantification and data analysis were performed using the iQ5 Real-Time PCR Detection System (Bio-Rad). The detection limit of this assay was 400-copies/ml plasma.

3. Results

3.1. Growth properties of prototype HIV-1mt clone, NL-DT5R in macaques in vitro and in vivo

We first examined the replication properties of prototype HIV-1mt NL-DT5R in $CD8^+$ cell-depleted PBMCs of CM and RM. NL-DT5R replicated in the cells of CM but not in those of RM (Fig. 2). We next examined the in vivo replication properties of NL-DT5R in CM. Viral stocks for inoculation were prepared with $CD8^+$ cell-depleted CM PBMCs as described above. Then, two monkeys were infected with NL-DT5R intravenously and bled periodically. As shown in Fig. 3A, NL-DT5R established infection as indicated by detectable levels of plasma viremia and an anti-HIV-1 antibody response, although the viral level was marginal (about 1×10^3 copies/ml) and disappeared at 4 weeks post infection.

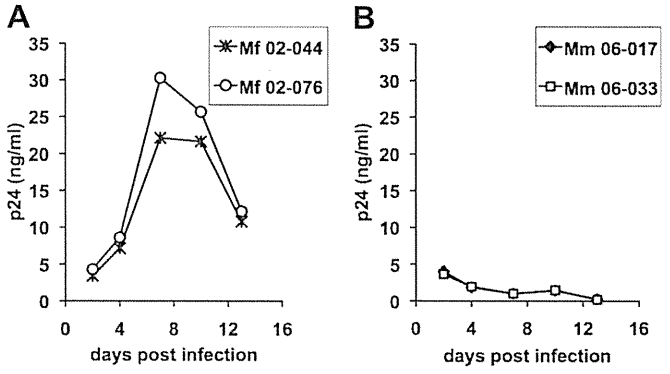

Fig. 2. Growth properties of the NL-DT5R in $CD8^+$ cell-depleted PBMCs from CM (A) and RM (B). The cells were infected with NL-DT5R and the viral replication was monitored by p24 antigen in the culture supernatants using a p24 quantitative ELISA kit. Animal identifications are indicated at the top of each panel.

These results indicated that although CM appeared permissive for NL-DT5R as compared with RM, the mutations introduced in NL-DT5R were not still sufficient to overcome the restriction by host factor(s) of these macaques.

3.2. MN4-5S showed improved replication capability in CM $CD8^+$ cell-depleted PBMCs

In order to improve the replication capability of HIV-1mt in CM, we conducted long-term passage of NL-DT5R in HSC-F cells. Additionally, NL-DT562, having an R5-tropic *env* gene on a background of NL-DT5R, was also passaged long-term in HSC-F cells. We found that the passaging improved the growth of the viruses (data not shown), and then viral clones were obtained after the long-term passaging and sequenced. Ten nucleotide substitutions were identified in the NL-DT5R-derived clone and 4 nucleotide substitutions (except for the *env* gene) in the NL-DT562-derived clone. These 14 nucleotide substitutions (7 of which were non-synonymous mutations) were assembled and introduced into NL-DT5R. The resultant clone was named MN4-5, and its structure is shown in Fig. 1. We previously found that insertion of an SIVmac loop between alpha helices 6 and 7 (L6/7) of CA into the corresponding region in HIV-1 significantly enhanced the viral replication in HSC-F cells and PBMCs of CM by relieving the inhibitory effect of TRIM5α [18]. We therefore inserted an SIVmac-derived L6/7 sequence into MN4-5. The resultant clone was named MN4-5S (Fig. 1). In order to examine the impact of these modifications on the viral replication, we analyzed the replication properties of this "adapted" virus in HSC-F cells and $CD8^+$ cell-depleted PBMCs of CM. MN4-5 showed higher replication as compared with NL-DT5R in both types of cells (Figs. 4 and 5). Moreover, MN4-5S showed enhanced growth capability in the cells as compared with the parental clones, NL-DT5R and MN4-5 (Figs. 4 and 5).

Notably, MN4-5S did not show any replication in RM cells (data not shown), indicating that the combination of the mutations introduced in NL-DT5R may be effective for escape from the restriction in CM cells but not in RM cells.

3.3. MN4-5S induced greater viremia in CM as compared with parental clone, NL-DT5R

Since MN4-5S showed enhanced ability to replicate in CM cells, we next examined the viral replication in vivo. The stock of MN4-5S virus was inoculated into 3 CM. MN4-5S induced 10-fold higher viremia in infected animals at 2–3 weeks after infection (Fig. 6A), as compared with that induced by NL-DT5R (see Fig. 3). This result was consistent with the in vitro result (Fig. 5) and demonstrated that the mutations inserted into NL-DT5R contributed to enhancement of viral replication in vivo. In addition, at the acute phase of infection a slight decrease of $CD4^+$ T cells was observed (Fig. 6B). The viremia became undetectable at 6 weeks after infection.

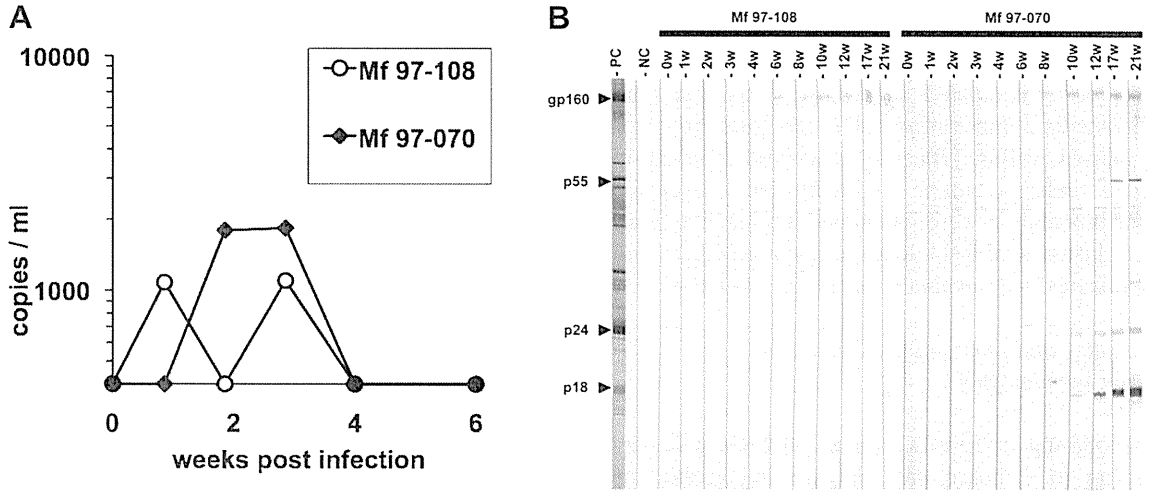

Fig. 3. Profiles of plasma viral RNA loads (A) and anti-HIV-1 antibody responses (B) in CM infected with NL-DT5R. Mf97-108 (open circles) and Mf97-070 (closed diamonds) were used in this study. Viral stocks for inoculation were prepared in $CD8^+$ cell-depleted PBMCs, and then 6.1 ng p24 of HIV-1 were inoculated into each animal. Commercially available diagnostic HIV-1 Western blotting strips were reacted with 100-fold diluted monkey plasma. Plasma from HIV-1-infected or uninfected individuals was used as a positive or a negative control, respectively.

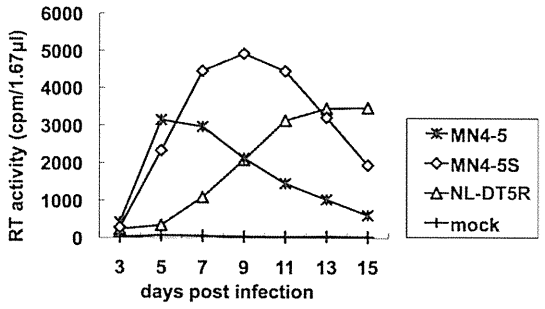

Fig. 4. Growth properties of HIV-1mt in HSC-F cells. The cells were infected with a series of HIV-1mt derivatives. The viral replication was monitored by RT activity in the culture supernatants.

Thereafter, antibody response against MN4-5S was observed in infected animals (Fig. 6C). As indicated by comparison with the lane of the positive control as a standard, the degree of antibody response seemed to be stronger than that against NL-DT5R (see Figs. 3B and 6C). Next we attempted to clarify the role of $CD8^+$ lymphocytes in the disappearance of viremia. We conducted in vivo depletion of $CD8^+$ cells by using a method reported previously [23]. We found that the reappearance of viremia was observed in all monkeys tested in parallel with the decline of $CD8^+$ T cells after the anti-CD8 mAb administration (Fig. 6A and D). This result indicated that $CD8^+$ T cells had a critical role in the control of HIV-1mt replication and suggested that the virus was able to infect latently in vivo.

4. Discussion

In the present study, we found that a modified HIV-1mt, MN4-5S, acquired greater ability to replicate in CM than NL-DT5R, and that both the SIVmac-derived L6/7 (HNP120-122 > RQQN120-123 of CA) and a series of substitutions identified by long-term passage of NL-DT5R in HSC-F cells contributed to this ability (Fig. 1). We recently showed that the substitution of L6/7 relieved the inhibitory effect of TRIM5α [18]. Additionally, our preliminary data suggest that non-synonymous mutations in the *integrase* and *env* genes are likely to be critical for the improved activity (Nomaguchi et al., manuscript in preparation). It is possible that these adaptive mutations may optimize the interaction between host and viral proteins.

It seemed that the growth kinetics of NL-DT5R in PM were comparable with those of MN4-5S in CM, which had peak levels in acute viremia of approximately 10^4 copies/ml [17]. It is therefore likely that PM may exhibit better susceptibility to HIV-1mt than CM. It is possible that the greater susceptibility of PM to HIV-1mt replication could be due to the genotype of TRIM5, because PM usually expresses a chimera between TRIM5α and CypA, so-called TRIM-Cyp, whose anti-HIV-1 activity is defective [24].

One unexpected finding in this study was that MN4-5S was unable to replicate in PBMCs of RM (data not shown), which was in contrast with the greater susceptibility of RM to SIV-mac infection. Our results suggested that RM was most resistant to HIV-1mt replication among the three macaque species. Since our HIV-1mt clones (NL-DT5R and MN4-5) were established on the basis of information obtained from serial passages of the viruses in CM-derived cells, it may be reasonable to consider that these viruses were consequently optimized to CM. Alternatively, it is also possible that anti-HIV-1 activities such as TRIM5α and APOBEC3 of RM could be greater than those of other macaques. Further studies are in progress to address these questions.

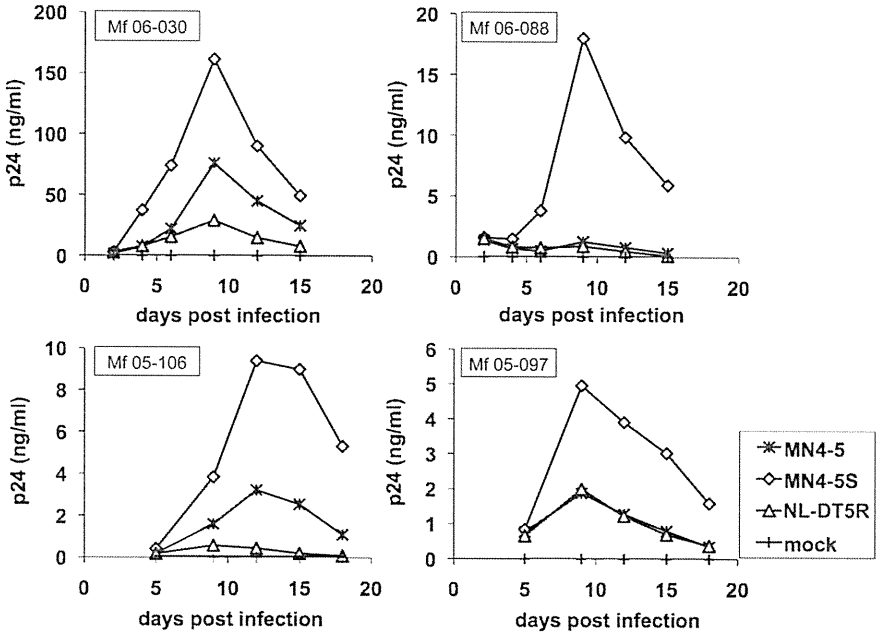

Fig. 5. Growth properties of HIV-1mt in $CD8^+$ cell-depleted PBMCs from four CM. The cells were infected with a series of HIV-1mt derivatives. The viral replication was monitored by p24 antigen in the culture supernatants using a p24 quantitative ELISA kit. Animal identifications are indicated at the top of each panel.

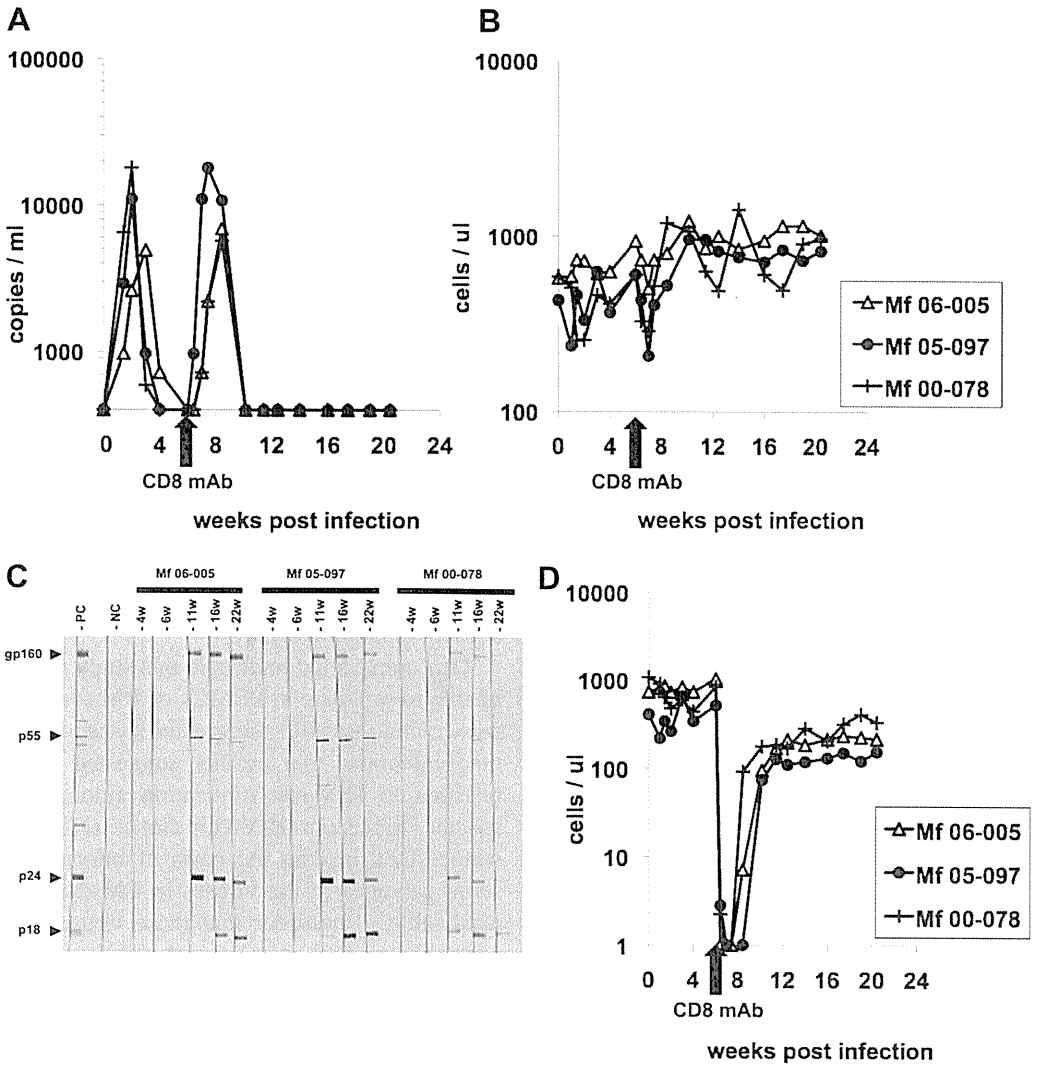

Fig. 6. Profiles of plasma viral RNA loads (A), circulating $CD4^+$ T lymphocytes (B), anti-HIV-1 antibody responses (C) and circulating $CD8^+$ T lymphocytes (D) in CM infected with HIV-1 derivatives. Viral stocks for inoculation were prepared in $CD8^+$ cell-depleted PBMCs and then 10 ng of p24 of HIV-1 were inoculated into each animal. Commercially available diagnostic HIV-1 Western blotting strips were reacted with 100-fold diluted plasma of each monkey. Plasma from HIV-1 infected or uninfected individuals was used as a positive or negative control, respectively. The black arrow indicates the day of anti-CD8 mAb (cM-T807) inoculation.

We demonstrated that the reappearance of viremia was observed in all monkeys tested in parallel with decline of $CD8^+$ T cells after anti-CD8 mAb administration (Fig. 6A and D). This result indicated that HIV-1-specific $CD8^+$ T cells had a critical role in the control of HIV-1mt replication and suggested that the virus may be able to infect latently in vivo. In order to establish a set point viremia and persistent infection, further modifications of HIV-1mt may be required to enable potent escape from the anti-viral immune response.

Further mechanistic characterization of anti-HIV-1 restriction factors will help in the construction of highly replicative and pathogenic HIV-1mt clones. As in the case of SHIV, in vivo passage of the virus could be a conventional and straightforward procedure for achieving such purposes [4]. However, the results of our study demonstrate that selective modification of HIV-1mt based on available knowledge regarding the molecular machineries is an alternative and powerful way. We are now in the process of developing the next generation of HIV-1mt that will acquire growth ability and pathogenicity in macaques as well as in humans.

Acknowledgements

The authors wish to thank T. Kurosawa, M. Fujita and M. Yasue for their helpful assistance. The authors also thank F. Ono, Y. Katakai, K. Komatsuzaki, A. Hiyaoka, K. Ohto, H. Ohto, and Y. Emoto for their support in animal experiments. We also thank M. Kaizu for his technical support. The anti-CD8 antibody used in the present study was provided by the NIH Nonhuman Primate Reagent Resource (R24 RR016001, N01 AI040101). This work was supported by grants from the Japan Health Sciences Foundation and the Ministry of Health, Labor, and Welfare in Japan and by Global COE Program A06 of Kyoto University.

References

[1] N.L. Letvin, M.D. Daniel, P.K. Sehgal, R.C. Desrosiers, R.D. Hunt, L.M. Waldron, J.J. MacKey, D.K. Schmidt, L.V. Chalifoux, N.W. King, Induction of AIDS-like disease in macaque monkeys with T-cell tropic retrovirus STLV-III, Science 230 (1985) 71–73.

[2] H. Kestler, T. Kodama, D. Ringler, M. Marthas, N. Pedersen, A. Lackner, D. Regier, P. Sehgal, M. Daniel, N. King, et al., Induction of AIDS in rhesus monkeys by molecularly cloned simian immunodeficiency virus, Science 248 (1990) 1109–1112.

[3] R. Shibata, M. Kawamura, H. Sakai, M. Hayami, A. Ishimoto, A. Adachi, Generation of a chimeric human and simian immunodeficiency virus infectious to monkey peripheral blood mononuclear cells, J. Virol. 65 (1991) 3514–3520.

[4] K.A. Reimann, J.T. Li, R. Veazey, M. Halloran, I.W. Park, G.B. Karlsson, J. Sodroski, N.L. Letvin, A chimeric simian/human immunodeficiency virus expressing a primary patient human immunodeficiency virus type 1 isolate env causes an AIDS-like disease after in vivo passage in rhesus monkeys, J. Virol. 70 (1996) 6922–6928.

[5] M. Nomaguchi, N. Doi, K. Kamada, A. Adachi, Species barrier of HIV-1 and its jumping by virus engineering, Rev. Med. Virol. 18 (2008) 261–275.

[6] D. Sauter, A. Specht, F. Kirchhoff, Tetherin: holding on and letting go, Cell 141 (2010) 392–398.

[7] M. Stremlau, C.M. Owens, M.J. Perron, M. Kiessling, P. Autissier, J. Sodroski, The cytoplasmic body component TRIM5alpha restricts HIV-1 infection in Old World monkeys, Nature 427 (2004) 848–853.

[8] E.E. Nakayama, T. Shioda, Anti-retroviral activity of TRIM5 alpha, Rev. Med. Virol. 20 (2010) 77–92.

[9] A.M. Sheehy, N.C. Gaddis, J.D. Choi, M.H. Malim, Isolation of a human gene that inhibits HIV-1 infection and is suppressed by the viral Vif protein, Nature 418 (2002) 646–650.

[10] S. Henriet, G. Mercenne, S. Bernacchi, J.C. Paillart, R. Marquet, Tumultuous relationship between the human immunodeficiency virus type 1 viral infectivity factor (Vif) and the human APOBEC-3G and APOBEC-3F restriction factors, Microbiol. Mol. Biol. Rev. 73 (2009) 211–232.

[11] M.H. Malim, APOBEC proteins and intrinsic resistance to HIV-1 infection, Philos. Trans. R Soc. Lond B. Biol. Sci. 364 (2009) 675–687.

[12] S.J. Neil, T. Zang, P.D. Bieniasz, Tetherin inhibits retrovirus release and is antagonized by HIV-1 Vpu, Nature 451 (2008) 425–430.

[13] J.L. Douglas, J.K. Gustin, K. Viswanathan, M. Mansouri, A.V. Moses, K. Fruh, The great escape: viral strategies to counter BST-2/tetherin, PLoS Pathog. 6 (2010) e1000913.

[14] R. Mariani, D. Chen, B. Schrofelbauer, F. Navarro, R. Konig, B. Bollman, C. Munk, H. Nymark-McMahon, N.R. Landau, Species-specific exclusion of APOBEC3G from HIV-1 virions by Vif, Cell 114 (2003) 21–31.

[15] B. Jia, R. Serra-Moreno, W. Neidermyer, A. Rahmberg, J. Mackey, I.B. Fofana, W.E. Johnson, S. Westmoreland, D.T. Evans, Species-specific activity of SIV Nef and HIV-1 Vpu in overcoming restriction by tetherin/BST2, PLoS Pathog. 5 (2009) e1000429.

[16] K. Kamada, T. Igarashi, M.A. Martin, B. Khamsri, K. Hatcho, T. Yamashita, M. Fujita, T. Uchiyama, A. Adachi, Generation of HIV-1 derivatives that productively infect macaque monkey lymphoid cells, Proc Natl Acad Sci U S A 103 (2006) 16959–16964.

[17] T. Igarashi, R. Iyengar, R.A. Byrum, A. Buckler-White, R.L. Dewar, C. E. Buckler, H.C. Lane, K. Kamada, A. Adachi, M.A. Martin, Human immunodeficiency virus type 1 derivative with 7% simian immunodeficiency virus genetic content is able to establish infections in pig-tailed macaques, J. Virol. 81 (2007) 11549–11552.

[18] A. Kuroishi, A. Saito, Y. Shingai, T. Shioda, M. Nomaguchi, A. Adachi, H. Akari, E.E. Nakayama, Modification of a loop sequence between alpha-helices 6 and 7 of virus capsid (CA) protein in a human immunodeficiency virus type 1 (HIV-1) derivative that has simian immunodeficiency virus (SIVmac239) vif and CA alpha-helices 4 and 5 loop improves replication in cynomolgus monkey cells, Retrovirology 6 (2009) 70.

[19] A. Adachi, H.E. Gendelman, S. Koenig, T. Folks, R. Willey, A. Rabson, M.A. Martin, Production of acquired immunodeficiency syndrome-associated retrovirus in human and nonhuman cells transfected with an infectious molecular clone, J. Virol. 59 (1986) 284–291.

[20] T. Yamashita, N. Doi, A. Adachi, M. Nomaguchi, Growth ability in simian cells of monkey cell-tropic HIV-1 is greatly affected by downstream region of the vif gene, J. Med. Invest. 55 (2008) 236–240.

[21] H. Akari, K.H. Nam, K. Mori, I. Otani, H. Shibata, A. Adachi, K. Terao, Y. Yoshikawa, Effects of SIVmac infection on peripheral blood CD4+CD8+ T lymphocytes in cynomolgus macaques, Clin. Immunol. 91 (1999) 321–329.

[22] R.L. Willey, D.H. Smith, L.A. Lasky, T.S. Theodore, P.L. Earl, B. Moss, D.J. Capon, M.A. Martin, In vitro mutagenesis identifies a region within the envelope gene of the human immunodeficiency virus that is critical for infectivity, J. Virol. 62 (1988) 139–147.

[23] J.E. Schmitz, M.A. Simon, M.J. Kuroda, M.A. Lifton, M.W. Ollert, C.W. Vogel, P. Racz, K. Tenner-Racz, B.J. Scallon, M. Dalesandro, J. Ghrayeb, E.P. Rieber, V.G. Sasseville, K.A. Reimann, A nonhuman primate model for the selective elimination of CD8+ lymphocytes using a mouse-human chimeric monoclonal antibody, Am. J. Pathol. 154 (1999) 1923–1932.

[24] C.A. Virgen, Z. Kratovac, P.D. Bieniasz, T. Hatziioannou, Independent genesis of chimeric TRIM5-cyclophilin proteins in two primate species, Proc. Natl. Acad. Sci. U S A 105 (2008) 3563–3568.

Immunogenetics (2011) 63:417–428
DOI 10.1007/s00251-011-0519-7

ORIGINAL PAPER

Molecular evolution of immunoglobulin superfamily genes in primates

Hitoshi Ohtani · Toshiaki Nakajima · Hirofumi Akari · Takafumi Ishida · Akinori Kimura

Received: 1 September 2010 / Accepted: 17 February 2011 / Published online: 10 March 2011

Abstract Genes of the immunoglobulin superfamily (IgSF) have a wide variety of cellular activities. In this study, we investigated molecular evolution of IgSF genes in primates by comparing orthologous sequences of 249 IgSF genes among human, chimpanzee, orangutan, rhesus macaque, and common marmoset. To evaluate the non-synonymous/synonymous substitution ratio (ω), we applied Bn-Bs program and PAML program. IgSF genes were classified into 11 functional categories based on the Gene Ontology (GO) database. Among them, IgSF genes in three functional categories, immune system process (GO:0002376), defense response (GO:0006952), and multi-organism process (GO:0051704), which are tightly linked to the regulation of immune system had much higher values of ω than genes in the other GO categories. In addition, we estimated the average values of ω for each primate lineage. Although each primate lineage had comparable average values of ω, the human lineage showed the lowest ω value for the immune-related genes. Furthermore, 11 IgSF genes, *SIGLEC5*, *SLAMF6*, *CD33*, *CD3E*, *CEACAM8*, *CD3G*, *FCER1A*, *CD48*, *CD4*, *TIM4*, and *FCGR2A*, were implied to have been under positive selective pressure during the course of primate evolution. Further sequence analyses of *CD3E* and *CD3G* from 23 primate species suggested that the Ig domains of *CD3E* and *CD3G* underwent the positive Darwinian selection.

Keywords Natural selection · Immune system · Immunoglobulin domain · Comparative genomics · CD3 complex

Electronic supplementary material The online version of this article (doi:10.1007/s00251-011-0519-7) contains supplementary material, which is available to authorized users.

H. Ohtani · T. Nakajima · A. Kimura (✉)
Department of Molecular Pathogenesis, Medical Research Institute, and Laboratory of Genome Diversity, Graduate School of Biomedical Science, Tokyo Medical and Dental University, 1-5-45 Yushima, Bunkyo-ku, Tokyo 113–8510, Japan
e-mail: akitis@mri.tmd.ac.jp

H. Akari
Center for Human Evolution Modeling Research, Primate Research Institute, Kyoto University, Inuyama, Japan

T. Ishida
Unit of Human Biology and Genetics, Graduate School of Science, The University of Tokyo, Tokyo, Japan

Introduction

Comparative genomics is a promising approach for studying the biological development of the genome from the view point of evolution. Recently, large-scale genome sequences of human, chimpanzee, orangutan, rhesus macaque, and common marmoset have been made available (Consortium CSaA 2005; Gibbs et al. 2007), and the comparative genomic analyses among primates are crucial for addressing the issue of which genetic changes have made us uniquely human. In addition, such analyses are also useful for identifying the susceptibility genes for human diseases and for understanding the pathophysiological mechanisms of the diseases, because the biological differences among primates, such as differences in the disease susceptibility, have been reported (Lyashchenko et al. 2008; Song et al. 2005).

To identify the genes that have come under the pressure of natural selection in the course of primate evolution is of critical importance, because such genes would very likely be linked to biological function involved in the human

diseases. In fact, comparisons of genomes between the human and chimpanzee and between the human and rhesus macaque have suggested that dozens of genes have emerged under the pressure of natural selection in the course of primate evolution, in particular, those which are involved in the host–pathogen interactions, reproduction, and sensory systems (Clark et al. 2003; Gibbs et al. 2007; Nielsen et al. 2005). These studies have also reported that the immunoglobulin superfamily (IgSF) genes are commonly observed among the genes in primates, which had come under the pressure of natural selection.

Members of the IgSF are defined by the presence of one or more regions homologous to the basic structural unit of immunoglobin (Ig) molecules. The Ig domain possesses a characteristic Ig fold, which is composed of two opposing anti-parallel beta-strands connected by disulfide bonds between cysteine residues (Halaby and Mornon 1998). The IgSF is a large group of cell surface, cytoplasmic, and serum proteins involved in the recognition, binding, and/or adhesion processes of cells (Lander et al. 2001). Members of the IgSF have a wide variety of cellular functions acting as cell surface antigen receptors, co-receptors and co-stimulatory molecules of the immune system, molecules involved in antigen presentation to lymphocytes, cell adhesion molecules, certain cytokine receptors, and intracellular muscle proteins. They are commonly ascribed to a role in molecular–molecular interactions (Barclay 2003; Lander et al. 2001; Otey et al. 2009).

Although the IgSF genes have been reported as showing evidence of positive selection, the phylogenetic analyses focused on the Ig domains of IgSF genes have not been conducted. The purpose of present study is to provide insights into the overview of the molecular evolution of the IgSF genes and to identify the IgSF genes under the positive selection in the course of five primate species.

Materials and methods

Sequence data collection

Selection of the IgSF genes was done by using the Conserved Domain Database v2.22 at the National Center for Biotechnology Information (NCBI) (http://www.ncbi.nlm.nih.gov/sites/entrez). As in the previous studies (Gibbs et al. 2007; Kosiol et al. 2008), we identified orthologous genes for human IgSF genes from chimpanzee, orangutan, rhesus macaque, and common marmoset by using the UCSC/MULTIZ alignment program which is constructed by the synteny-based genome-wide multiple alignments (Blanchette et al. 2004; Kent et al. 2003). Sequence alignment was done by using the Clustal X program (Larkin et al. 2007). IgSF genes were classified based on the Gene Ontology (GO) database (http://www.geneontology.org/) (Ashburner et al. 2000).

Primate genomic DNA samples

DNA samples from 23 primate species including human (*Homo sapiens*), chimpanzee (*Pan troglodytes*), bonobo (*Pan paniscus*), gorilla (*Gorilla gorilla*), orangutan (*Pongo pygmaeus*), black gibbon (*Hylobates concolor*), white-handed gibbon (*Hylobates lar*), siamang (*Symphalangus syndactylus*), rhesus macaque (*Macaca mulatta*), crab-eating macaque (*Macaca fascicularis*), baboon (*Papio hamadryas*), black and white colobus (*Colobus guereza*), dusky lutong (*Trachypithecus obscurus*), silvered lutong (*Trachypithecus cristatus*), Central American spider monkey (*Ateles geoffroyi*), long-haired spider monkey (*Ateles belzebuth*), tufted capuchin (*Cebus apella*), common squirrel monkey (*Saimiri sciureus*), red-handed tamarin (*Saguinus midas*), cotton-top tamarin (*Saguinus oedipus*), golden lion tamarin (*Leonthopithecus rosalia*), common marmoset (*Callithrix jacchus*), and lesser galago (*Galago senegalensis*) were analyzed for *CD3E* and *CD3G* sequences.

PCR and sequencing analysis of *CD3E* and *CD3G*

Sequence information for coding regions of *CD3E* and *CD3G* were obtained by direct sequencing of gene segments amplified by polymerase chain reaction (PCR) from the genomic DNA samples. Primers for PCR were designed in the highly conserved non-coding regions among the genes from human, chimpanzee, orangutan, rhesus macaque, and common marmoset, referring the genomic sequences deposited in the UCSC Genome Browser (electronic supplementary material (ESM) Table 1). Primers for prosimian were designed by referencing the common marmoset sequences and whole-genome shotgun sequences from prosimians in NCBI BLAST (http://blast.ncbi.nlm.nih.gov/Blast.cgi). The primers were used for both PCR and direct sequencing analyses of the genes. When sequence variations (heterozygous sequences) in specific species were detected, the sequences which were conserved among 23 primate species were considered as ancestral sequences and used in the statistical analyses.

PCR was performed in a reaction mixture of 15 μL containing 0.1 μL Taq DNA polymerase (Takara Bio Inc., Shiga, Japan), 1 μL of 50 ng/μL DNA template, 1.5 μL of 2.0 mM dNTPs, 0.5 μL of 10 μM each primer, 1.5 μL reaction buffer containing 20 mM $MgCl_2$, and sterile water. PCR condition was as follows: 94°C for 2 min, 35 cycles (94°C for 30 s, 55–60°C for 30 s, 72°C for 1 min), and 72°C for 5 min. PCR products were then purified and sequenced by the BigDye Terminator cycling system using an ABI3130× automated DNA sequencer (Applied Biosystems,

Foster City, CA, USA). Editing and assembly of sequences were performed using SEQUENCHER (Gene Codes, Ann Arbor, MI, USA). The *CD3E* and *CD3G* sequences determined in this study were deposited in DNA Data Bank of Japan under the following accession numbers: AB583139-AB583171 (ESM Table 2).

Statistical analyses

In this study, we used both Bn-Bs program and PAML program to reduce the chance of false-positive findings. A criterion for the gene under positive selection pressure was that the p values obtained by both the Bn-Bs and PAML programs were less than 0.05. The first screening of IgSF genes under the selection pressure was performed by using the Bn-Bs program. The genes showing p values less than 0.05 in the first screening were further analyzed by using the PAML program.

The Bn-Bs program estimates the values of non-synonymous substitution rate (dn) and synonymous substitution rate (ds) based on the modified Nei–Gojobori method (Nei and Gojobori 1986), where a phylogenetic tree is given (Zhang et al. 1998). The value of ω, an abbreviation for the value of dn/ds, is a criterion of natural selective pressure acting on the gene. Statistical significance of the difference between dn and ds were examined by Z test (Chatterjee et al. 2009). An ordinary least-squares method was used to estimate the branch lengths and variances for the evolutionary distances between two sequences (Rzhetsky and Nei 1993).

Investigation on the presence of branch-specific positive selection (the branch model) and site-specific positive selection (the site model) were performed by using CODEML, an application from PAML version 4.7 (Yang 2007). The branch model is used for evaluation of difference in the value of ω for each branch, and it is useful for detecting a positive selection acting on particular branch by using the likelihood ratio tests (Yang and Nielsen 2000). The site model treats ω allowing the variance among codons (Yang 2005; Yang and Nielsen 2000). Bayes empirical Bayes (BEB) method was used to detect the sites under the positive selection (Yang and Nielsen 2000; Wong et al. 2004; Yang et al. 2005; Yang 2005, 2007).

Results

Non-synonymous/synonymous substitution ratio of IgSF genes

Four hundred sixty-one IgSF genes were selected from the human genome, based on the Conserved Domain Database v2.22 at NCBI (http://www.ncbi.nlm.nih.gov/Structure/cdd/cdd.shtml). Among them, 47 genes composed of MHC, KIR, and PSG genes (ESM Table 3) were excluded from the phylogenetic analysis, because there are many paralogous genes with high similarity in the sequences, which may lead to uncertainty to identify the reliable orthologous genes. Thus, a total of 414 IgSF genes were subjected to the following analysis. By using the UCSC Genome Browser (http://genome.ucsc.edu/), we attempted to identify orthologous genes for these 414 human IgSF genes in genomes from chimpanzee, orangutan, rhesus macaque, and common marmoset. We were unable to identify orthologs for 53, 55, 52, and 81 genes from the genome of chimpanzee, orangutan, rhesus macaque, and common marmoset, respectively, due to the alignment incompleteness (sequence identity of less than 80%), insertion/deletions accompanied by frameshift, or nucleotide substitutions resulting in a premature stop codon. After removing the IgSF genes of which the reliable orthologous genes were not identified in the non-human primates, remaining 249 IgSF genes were used in the study of positive selection.

The Bn-Bs program was applied to evaluate the non-synonymous/synonymous substitution ratio (Larkin et al. 2007), and the value of Σdn and Σds, which were the sum values of dn and ds, respectively, in seven primate lineages, human, chimpanzee, human-chimpanzee ancestor, orangutan, human–chimpanzee–orangutan ancestor, rhesus macaque, and common marmoset were calculated. The IgSF genes were classified into 11 functional categories based on the Gene Ontology database (http://www.geneontology.org/); GO:0002376: immune system process, GO:0006952: defense response, GO:0051704: multi-organism process, GO:0007166: cell surface receptor linked signaling pathway, GO:0007155: cell adhesion, GO:0007165: signal transduction, GO:0008219: cell death, GO:0030154 : cell differentiation, GO:0008283: cell proliferation, GO:0019222: regulation of metabolic process and GO:0050794: regulation of cellular process. When the Σdn/Σds ratios were calculated for the entire coding sequences, there was no evidence to support the presence of positive natural selection. The Σdn/Σds ratios from the analyzed genes, except for *LAIR1* (Σdn/Σds ratio= 1.00, statistically not significant), were lower than 1.0, implying that most of the IgSF genes had been under the pressure of negative selection in the course of primate evolution. Among the functional categories, GO:0002376: immune system process (median Σdn/Σds ratio=0.407; interquartile range (IQR), 0.285–0.632, $p=1.40\times10^{-6}$), GO:0006952: defense response (median Σdn/Σds ratio= 0.394; IQR, 0.287–0.506, $p=6.73\times10^{-3}$), and GO:0051704: multi-organism process (median Σdn/Σds ratio=0.400, IQR, 0.302–0.475, $p=2.46\times10^{-2}$) showed much higher values of Σdn/Σds ratio than the tested IgSF genes (median Σdn/Σds ratio=0.208, IQR, 0.107–0.440; Fig. 1a).

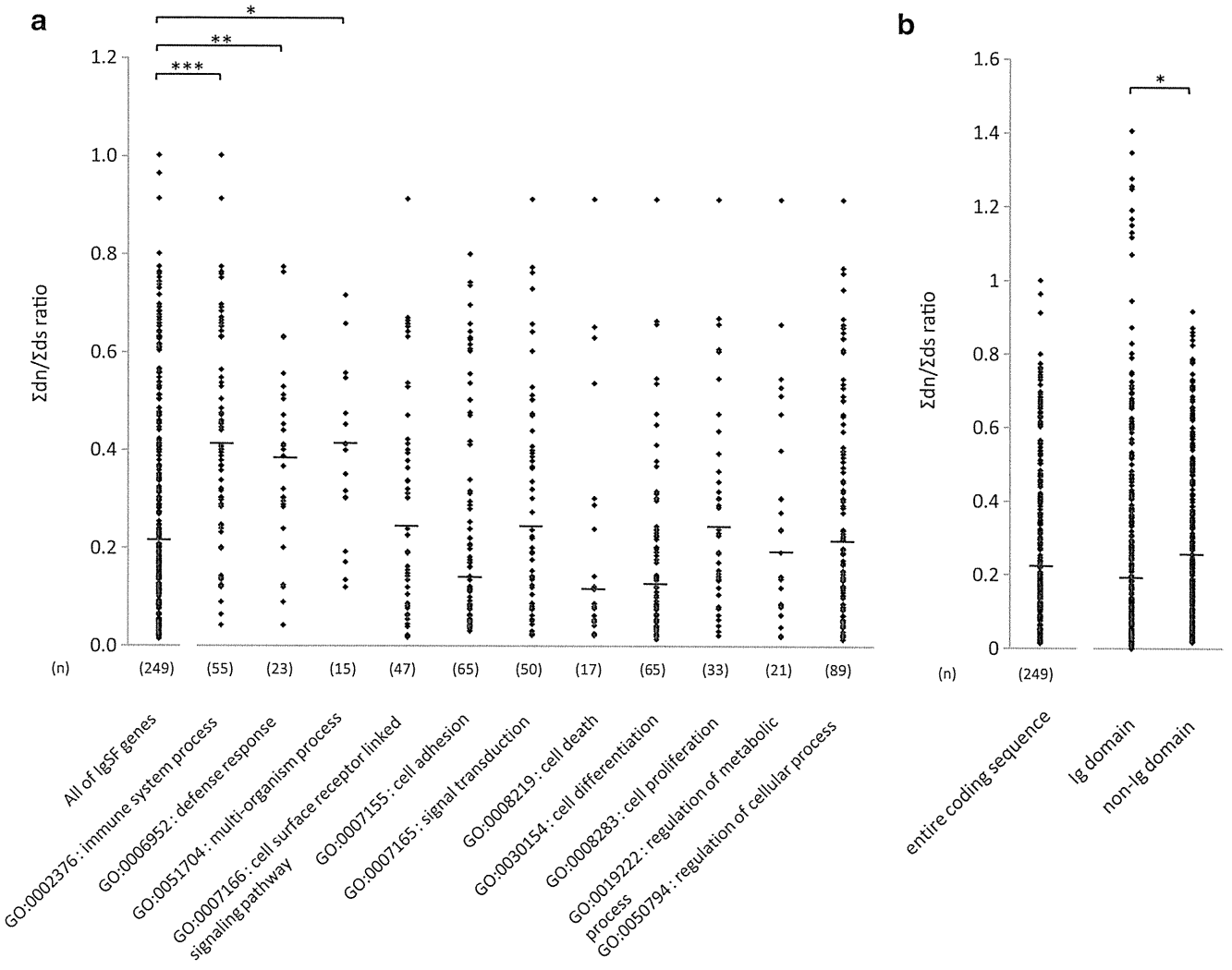

Fig. 1 Σdn/Σds ratio of IgSF genes. **a** The IgSF genes were categorized by gene ontology. **b** Σdn/Σds ratios for the entire coding region, Ig domain, and non-Ig domain. The Σdn/Σds ratios were calculated by Bn-Bs program. *Bars* indicate median values of Σdn/Σds ratio for each group. An *asterisk* indicates that there was significant difference between two groups (*$p<0.05$, **$p<0.01$, ***$p<0.001$)

The coding segments of IgSF genes were divided into two segments in each gene; one was the segment encoding the Ig domain, whereas the other was the coding region other than the Ig domain (non-Ig domain). The Σdn/Σds ratios were also separately calculated for the Ig and non-Ig domains in the IgSF genes. As shown in Fig. 1b, the Σdn/Σds ratios for the Ig domains (median Σdn/Σds ratio=0.198; IQR, 0.070–0.420) were significantly lower than the Σdn/Σds ratios for the non-Ig domains (median Σdn/Σds ratio=0.242; IQR, 0.125–0.456, $p=2.10\times10^{-2}$). Interestingly, despite the lower levels of Σdn/Σds ratio for the Ig domains, the Σdn/Σds ratios of Ig domains from 11 genes, *LAIR1*, *CD3G*, *CD3E*, *CEACAM7*, *ICAM4*, *CD244*, *CD4*, *CD3D*, *CD7*, *SLAMF6*, and *BTLA*, were over 1.0 and higher than mean Σdn/Σds of the non-Ig domains, although none of them was statistically significant.

Non-synonymous/synonymous substitution ratios of IgSF genes in primate lineages

Average values of ω for different lineages, including human, chimpanzee, orangutan, rhesus macaque, and common marmoset lineages, were calculated. First, we made a long sequence by connecting the coding sequences from all IgSF genes to calculate the average ω value, because there were many IgSF genes in which the ds was 0, which made it impossible to determine the exact value of ω. Then, the values of ω at intervals of approximately 20,000 bases were calculated. The average values of ω for each branch of the five-specie phylogeny were also calculated by using the Bn-Bs program. It was found that the average values of ω for the entire coding region was 0.241 in the human lineage, 0.277 in the chimpanzee lineage, 0.225 in the orangutan lineage, 0.234 in the rhesus

lineage, and 0.281 in the marmoset lineage. We also estimated the average value for the immune-related IgSF genes, i.e. the IgSF genes categorized into GO:0002376, GO:0006952, and GO:0051704, and the average value for the other IgSF genes; 0.285 and 0.225 in the human lineage, 0.381 and 0.236 in the chimpanzee lineage, 0.307 and 0.193 in the orangutan lineage, 0.370 and 0.181 in the rhesus lineage, and 0.473 and 0.206 in the marmoset lineage, respectively. In addition, essentially identical results were obtained by using the PAML program (ESM Figs. 1 and 2).

IgSF genes under the pressure of positive natural selection

The dn and ds values for the entire coding regions of IgSF genes in each lineage were calculated by using the Bn-Bs program and plotted in Fig. 2, where the genes with dn values higher than ds values were distributed in the upper diagonal portion. We performed statistical tests by using both the Bn-Bs and PAML programs. When a statistically significant level (p value less than 0.05) was obtained by the Bn-Bs program, further analyses by using the PAML program were done. As the results, five IgSF genes were suggested to have been under the significant positive selection; *SIGLEC5* [Z score=2.70 (p=0.003), chi-square value=5.32 (p=0.021)], and *SLAMF6* [Z score=1.69 (p=0.046), chi-square value=3.93 (p=0.048)] in the human lineage, *CD33* [Z score=2.43 (p=0.008), chi-square value=4.90 (p=0.027)] in the chimpanzee lineage, and *CD3E* [Z score=2.67 (p=0.004), chi-square value=9.04 (p=0.003)] and *CEACAM8* [Z score=2.08 (p=0.019), chi-square value=6.52 (p=0.011)] in the human–chimpanzee–orangutan ancestor lineage (Table 1). No gene under the significant control of positive selection was identified in the human–chimpanzee ancestor lineage, the orangutan lineage, the rhesus lineage, or the marmoset lineage. We also calculated the dn and ds values in the seven lineages for the Ig and non-Ig domains in the IgSF genes. Five genes, *CD3E*, *CD3G*, *FCER1A*, *CD48*, and *CD4*, and four genes, *SIGLEC5*, *TIM4*, *FCGR2A*, and *CD3E*, were suggested to be under the positive natural selection in the Ig and non-Ig domains, respectively (Table 1, ESM Figs. 3 and 4).

It should be noted here that we did not perform a multiple-test adjustment, such as a strict Bonferroni correction, and thus the levels of statistical significance were marginal. Nevertheless, we obtained significant results in the analyses done by two different programs, the Bn-Bs and PAML programs, instead of performing the multiple-test adjustment. In the Bn-Bs program, statistical significance of the difference between the dn and ds values were examined by Z test. On the other hand, in the PAML program, detection of positive selection acting on particular branch was based on the likelihood ratio test.

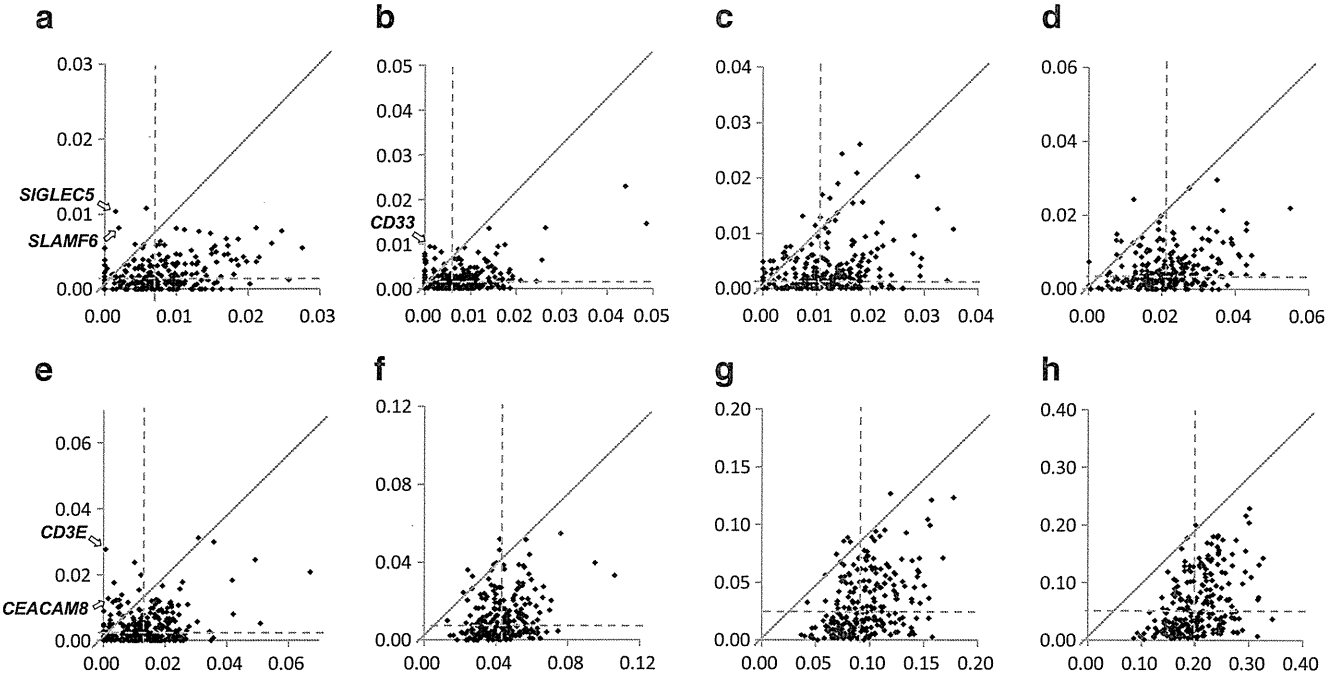

Fig. 2 Pairwise comparison plots of dn and ds values for the entire coding regions of IgSF genes in primate lineages. The values of dn (*vertical axis*) and ds (*horizontal axis*) for each primate lineage and their summation (Σ) were calculated by Bn-Bs program. *Dotted lines* indicate the average values of dn or ds. Arrows indicate the IgSF genes which were identified as to be under a positive selection by the analysis of both Bn-Bs and PAML program analyses. **a** Human lineage, **b** chimpanzee lineage, **c** human–chimpanzee ancestor lineage, **d** orangutan lineage, **e** human–chimpanzee–orangutan ancestor lineage, **f** rhesus lineage, **g** marmoset lineage, **h** Σ

Table 1 IgSF genes suggested to be under the positive selection in the course of primate evolution

Region	Gene name	Accession	BnBs			PAML			Lineage[c]
			ω (dn, ds)	*Z* score	*p* Value	ω	Chi-square	*p* Value	
Entire coding region	*SIGLEC5*	NM_003830	6.90 (0.010, 0.002)	2.70	0.003	nc	5.32	0.021	H
	SLAMF6	NM_052931	4.19 (0.008, 0.002)	1.68	0.046	nc	3.93	0.048	H
	FCGR3A	NM_000569	nc[a] (0.008, 0.000)	2.56	0.005	nc	2.80	ns[b]	C
	CD33	NM_001772	8.40 (0.009, 0.001)	2.43	0.008	nc	4.90	0.027	C
	TIM4	NM_138379	29.43 (0.006, 0.000)	2.12	0.017	nc	3.81	ns	C
	IL11RA	NM_001142784	nc (0.004, 0.000)	2.01	0.022	nc	2.24	ns	C
	FCGR2A	NM_021642	nc (0.004, 0.000)	1.99	0.023	nc	1.27	ns	C
	ICAM2	NM_000873	65.00 (0.006, 0.001>)	1.93	0.027	nc	2.16	ns	C
	AMICA1	NM_001098526	nc (0.004, 0.000)	1.77	0.039	nc	2.33	ns	C
	CD244	NM_001166663	4.34 (0.009, 0.002)	1.70	0.044	3.06	1.27	ns	C
	CD3E	NM_000733	48.67 (0.028, 0.001)	2.67	0.004	nc	9.03	0.003	HCO
	CEACAM8	NM_001816	8.73 (0.013, 0.001)	2.08	0.019	nc	6.52	0.011	HCO
	BTLA	NM_181780	5.30 (0.018, 0.003)	1.69	0.046	4.74	2.13	ns	HCO
Ig domain	*CD244*	NM_001166663	6.20 (0.022, 0.004)	1.96	0.025	nc	3.77	ns	H
	FCGR3A	NM_000569	19.98 (0.009, 0.001>)	1.89	0.029	nc	1.98	ns	H
	SLAMF6	NM_001184714	49.70 (0.011, 0.001>)	1.89	0.029	nc	1.95	ns	H
	CD244	NM_001166663	nc (0.017, 0.000)	2.51	0.006	nc	2.08	ns	C
	FCGR3A	NM_000569	nc (0.008, 0.000)	2.03	0.021	nc	1.69	ns	C
	BTN2A2	NM_006995	nc (0.007, 0.000)	1.77	0.038	nc	1.47	ns	C
	IGSF2	NM_004258	341.00 (0.007, 0.001>)	1.75	0.040	nc	2.35	ns	C
	VSIG10L	NM_001163922	nc (0.017, 0.000)	1.66	0.048	nc	0.63	ns	C
	LILRA4	NM_012276	nc (0.035, 0.000)	2.64	0.004	nc	2.50	ns	HC
	SLAMF6	NM_052931	nc (0.013, 0.000)	1.80	0.036	nc	2.58	ns	HC
	TIM4	NM_138379	206.00 (0.014, 0.000)	1.71	0.043	nc	1.11	ns	HC
	PECAM1	NM_000442	nc (0.009, 0.000)	2.31	0.010	nc	2.10	ns	O
	CEACAM7	NM_006890	292.40 (0.015, 0.000)	1.79	0.036	nc	1.75	ns	O
	BTLA	NM_181780	nc (0.025, 0.000)	2.43	0.008	nc	1.99	ns	HCO
	CD3E	NM_000733	16.07 (0.055, 0.003)	2.16	0.015	nc	4.43	0.035	HCO
	IGSF2	NM_004258	nc (0.009, 0.000)	1.76	0.039	nc	2.94	ns	HCO
	CD3G	NM_000073	nc (0.068, 0.000)	3.42	0.000	nc	4.74	0.029	R
	FCER1A	NM_002001	77.38 (0.029, 0.000)	2.86	0.002	nc	5.35	0.021	R
	ICAM4	NM_001544	nc (0.049, 0.000)	2.71	0.003	nc	2.89	ns	R
	CD3E	NM_000733	7.77 (0.085, 0.011)	2.62	0.004	nc	5.32	0.021	R
	SIGLEC11	NM_052884	2.08 (0.032, 0.015)	1.70	0.044	2.70	1.73	ns	R
	CD48	NM_001778	2.32 (0.197, 0.085)	2.31	0.010	2.65	4.23	0.040	M
	LRRC4	NM_022143	6.61 (0.051, 0.008)	1.79	0.037	3.59	1.69	ns	M
	CD4	NM_000616	1.92 (0.199, 0.104)	1.75	0.040	3.45	6.34	0.012	M
non-Ig domain	*SIGLEC5*	NM_003830	9.49 (0.012, 0.001)	2.66	0.004	nc	4.82	0.028	H
	TREML1	NM_178174	nc (0.005, 0.000)	1.75	0.040	nc	2.38	ns	H
	KAZALD1	NM_030929	nc (0.007, 0.000)	1.72	0.042	nc	1.72	ns	H
	CD33	NM_001772	24.03 (0.009, 0.001>)	2.17	0.015	nc	2.89	ns	C
	TIM4	NM_138379	27.66 (0.008, 0.001>)	2.09	0.018	nc	4.01	0.045	C
	IL11RA	NM_001142784	nc (0.005, 0.000)	1.79	0.037	nc	2.22	ns	C
	BTN1A1	NM_001732	52.71 (0.004, 0.001>)	1.72	0.043	nc	2.19	ns	C
	CD3E	NM_000733	154.60 (0.008, 0.001>)	1.67	0.047	nc	1.76	ns	HC
	SIRPB2	NM_001122962	10.29 (0.012, 0.001)	1.79	0.037	nc	2.89	ns	O
	FCGR2A	NM_021642	nc (0.017, 0.000)	2.64	0.004	nc	5.00	0.025	HCO
	CD3E	NM_000733	nc (0.017, 0.000)	1.66	0.048	nc	3.84	0.050	HCO

[a] *nc* Not calculated (Bs=0)

[b] *ns* Not significant ($p>0.05$)

[c] *H* human, *C* chimpanzee, *R* rhesus, *M* marmoset, *HC* human–chimpanzee ancestor, *HCO* human–chimpanzee–orangutan ancestor

Natural selection of *CD3E* and *CD3G* in primates

We further analyzed two genes, *CD3E* and *CD3G*, which were suggested to be under the positive natural selection. *CD3G* was the gene giving the lowest *p* value, and the Ig domain of CD3E underwent the positive selection. CD3E and CD3G tightly bound to each other (Xu et al. 2006). Because it is known that interacting protein pairs, such as receptor and its ligand, exhibit higher level of co-evolution than non-interacting protein pairs (Goh et al. 2000; Jothi et al. 2006; Li et al. 2005), we hypothesized that co-evolution might occur between *CD3E* and *CD3G*. To investigate the natural selection operated on these genes in the course of primate evolution, we determined protein coding sequences of *CD3E* and *CD3G* from 23 different primate species, including eight hominoids (human, chimpanzee, bonobo, gorilla, orangutan, black gibbon, white-handed gibbon, and siamang), six Old World monkeys (rhesus macaque, crab-eating macaque, hamadryas baboon, black and white colobus, silvered lutong, and dusky lutong), eight New World monkeys (common marmoset, cotton-top tamarin, red-handed tamarin, golden lion tamarin, common squirrel monkey, tufted capuchin, long-haired spider monkey, and Central American spider monkey), and one prosimian (lesser galago). After the alignment of nucleotide sequences and removal of alignment gaps, the values of dn and ds for the entire region, Ig domain, and non-Ig domain were calculated by using Bn-Bs program in each lineage of the phylogenic tree of primates.

The dn and ds values for *CD3E* in each primate lineage are indicated in Fig. 3. The dn values were larger than the ds values in several lineages which might be underwent positive selection pressure in the primate evolution. In particular, the dn values for the Ig domain were significantly

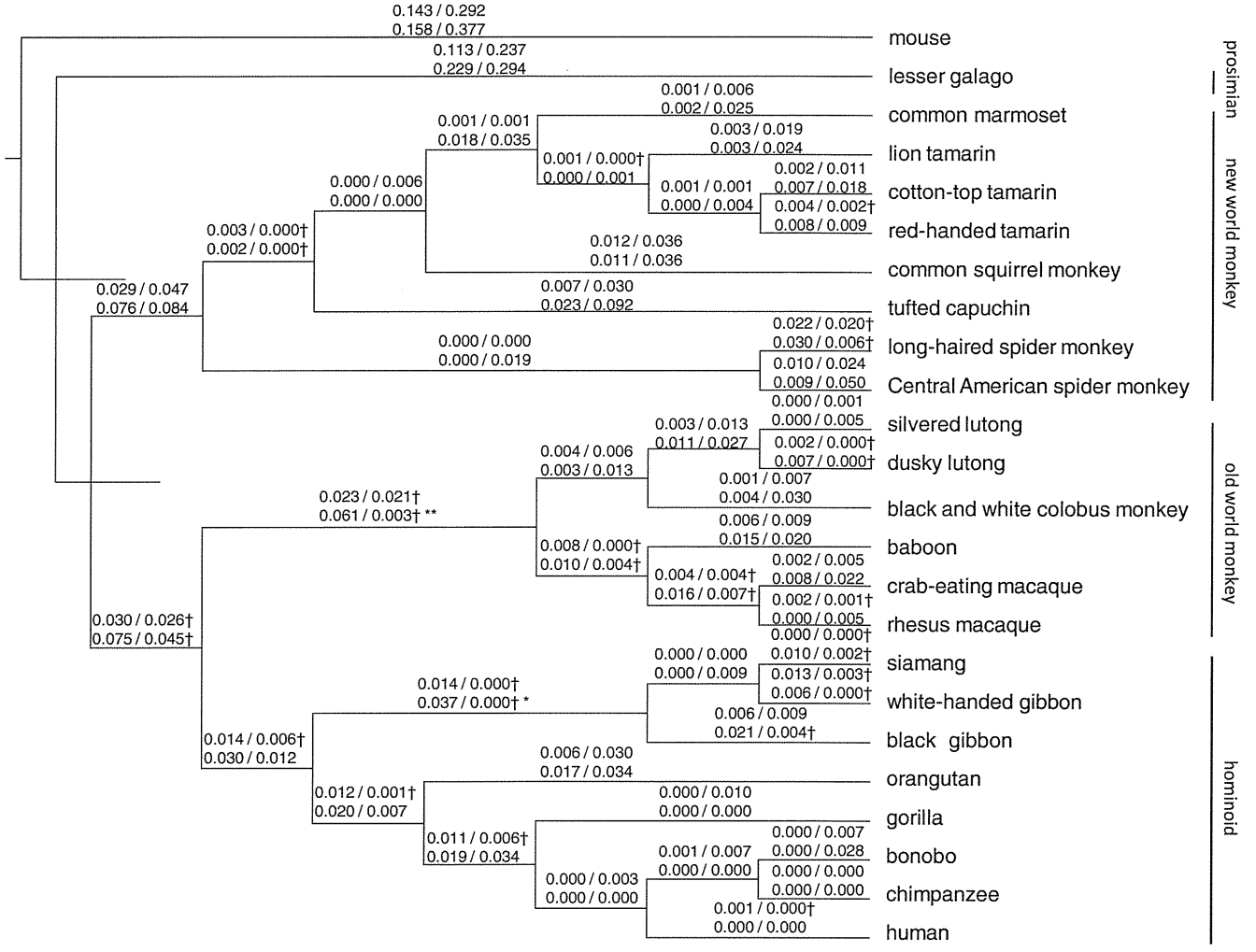

Fig. 3 Phylogenetic trees of *CD3E* in the primate evolution. *Values above branches* indicate estimated values of dn and ds per lineage by using Bn-Bs program. Values indicated in the upper parts are for the entire coding region, while values in the lower parts are for the Ig domain. *Daggers* indicate the value of dn higher than ds. An *asterisk* indicates that there was a significant difference between the dn and ds values (*$p<0.05$, **$p<0.01$, *Z* test)

larger than the ds values in two lineages: gibbon ancestor lineage [dn=0.061, ds=0.003, Z score=2.37 (p=0.009)] and Old World monkey ancestor lineage [dn=0.037, ds=0.000, Z score=1.94 (p=0.026)]. The significant positive selection on the Ig domains in the Old World monkey ancestor lineage [chi-square value=4.45 (p=0.035)] was confirmed by the PAML program, whereas it was not significant in the gibbon ancestor lineage [chi-square value=0.58 (p=0.446)]. Amino acid (AA) sequence alignment of CD3E in the primates is shown in Fig. 4. We identified three alignment gaps, all of which were in the Ig domain. Of 53 AAs of the Ig domain, approximately 30% (16/53) were evolutionary conserved among the primate species. On the other hand, approximately 70% (97/143) of AAs were conserved in the non-Ig domain, demonstrating that significantly more AA substitutions were distributed in the Ig domain ($p=2.16\times10^{-6}$). In addition, five AA sites in the Ig domain (positions at 51, 53, 72, 80, and 105 in the human sequence) were identified as possible target sites for the positive selection by the BEB method using the PAML program.

The dn and ds values for *CD3G* in each primate lineage were also measured by using the Bn-Bs program (ESM Fig. 5). The dn values for the Ig domain were significantly larger than the ds values in two lineages; Old World monkey ancestor lineage [dn=0.060, ds=0.000, Z score=3.30 (p=0.0005)] and hominoid and Old World monkey ancestor lineage [dn=0.042, ds=0.007, Z score=1.65 (p=0.049)]. The positive selection was confirmed by the PAML program in both lineages; Old World monkey ancestor lineage [chi-square value=5.32 (p=0.021)] and hominoid and Old World monkey ancestor lineage [chi-square value=4.17 (p=0.041)]. The AA alignment of CD3G from 23 primate species is shown in Fig. 4. Approximately 40% (25/56) of AAs in the Ig domain were conserved in the primate evolution, whereas

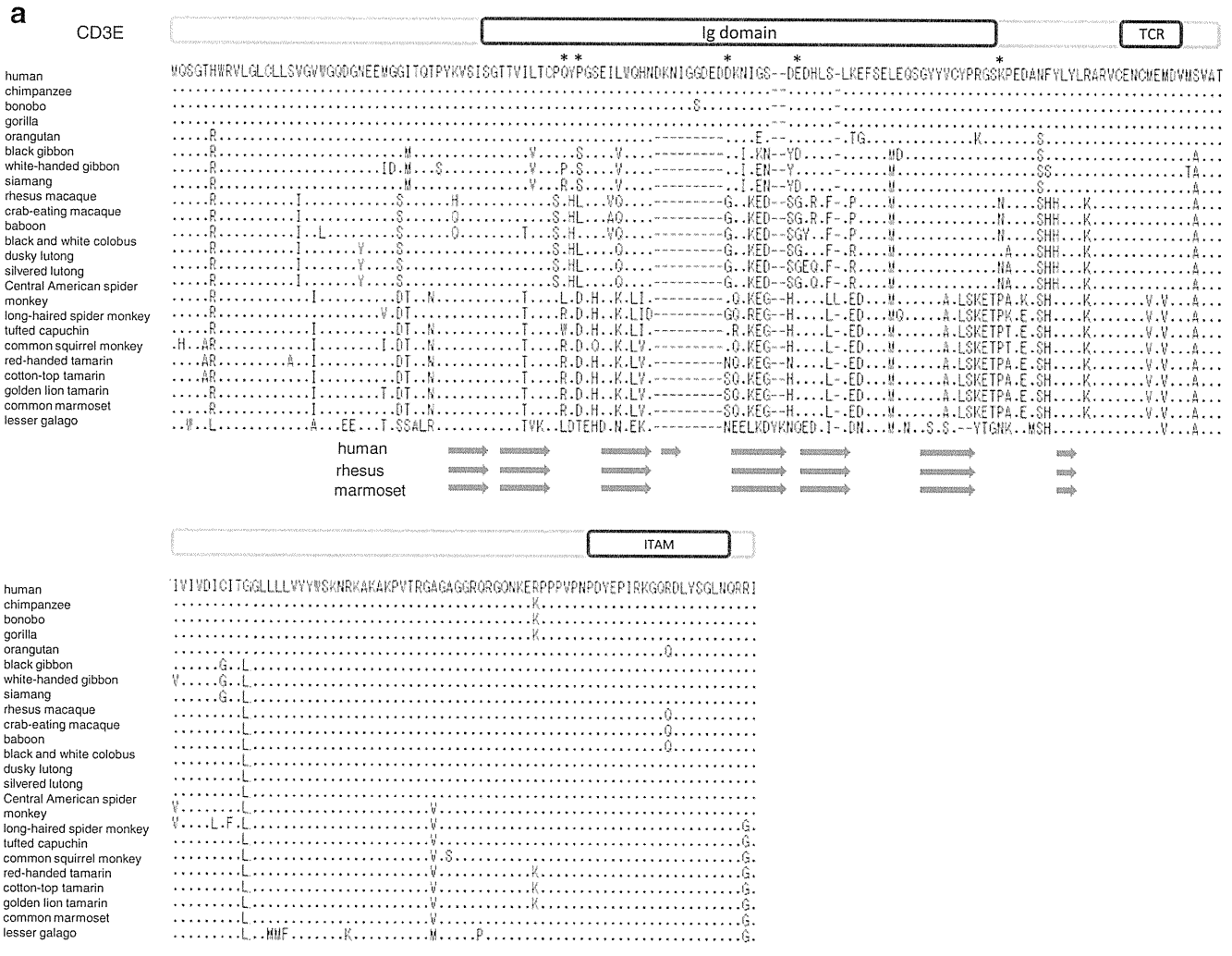

Fig. 4 Alignments of CD3E (**a**) and CD3G (**b**) amino acid sequences from 23 primate species. *Dots* indicate the identities to the human reference sequence, while hyphens indicate alignment gaps. TCR indicates amino acid sites at which the CD3 molecules interact with T cell receptor. ITAM represents the immune-tyrosine activation motif. *Arrows* indicated under the amino acid sequences are β-strand structures modeled by the SWISS-MODEL program. *Asterisks* indicate AA sites identified as being under the significant positive selection (p<0.05)

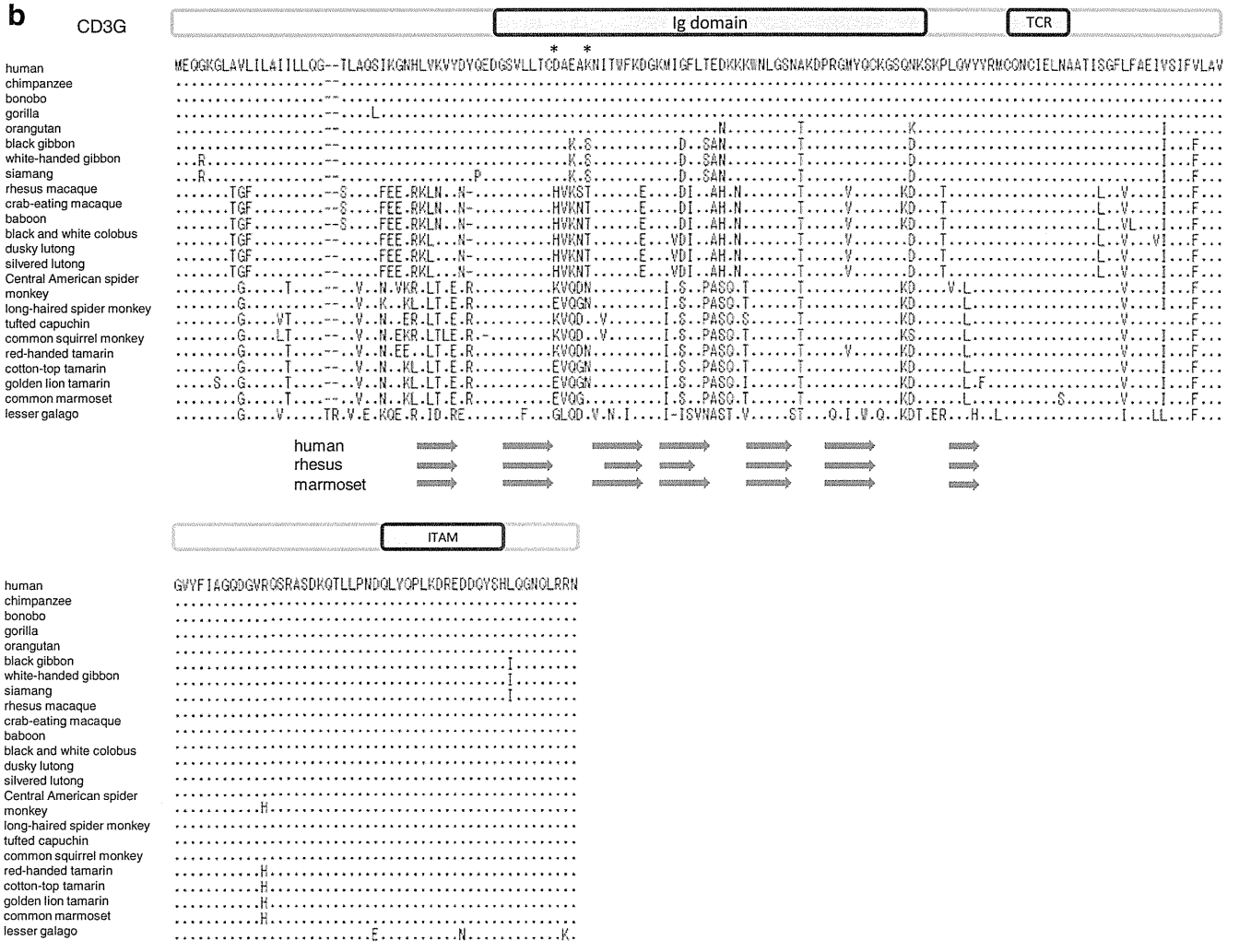

Fig. 4 (continued)

approximately 60% (81/128) of AAs in the non-Ig domain were conserved, demonstrating that the AA changes were significantly more frequent in the Ig domain (p=0.019). Two AA sites in the Ig domain (positions at 47 and 51 in the human sequence) were identified as significant target sites for the positive selection. These lines of evidence suggested that the pressure of positive Darwinian selection had shaped the structure of Ig domains in CD3E and CD3G during the course of primate evolution.

Discussion

Members of the IgSF have a wide variety of cellular activities and were classified into 11 functional categories based on the Gene Ontology database (http://www.geneontology.org/). When the association between the IgSF functional categories and the Σdn/Σds ratios were analyzed, three GO categories tightly linked to the immune system, i.e., GO:0002376: immune system process, GO:0006952: defense response, and GO:0051704: multi-organism process, showed much higher values for the Σdn/Σds ratio than the average value of the IgSF genes. It has been reported that the evolutionary rate of immune-related genes is higher than the other genes (Gibbs et al. 2007; Kosiol et al. 2008; Nielsen et al. 2005; Yu et al. 2006). The rapid evolution of immune-related genes might be a direct consequence of a complex selection pressure exerted by infectious diseases, autoimmunity, and tumors (Barreiro and Quintana-Murci 2010). On the other hand, as shown in Fig. 1a, the Σdn/Σds ratios of genes linked to three functional categories, GO:0007155: cell adhesion, GO:0007165: signal transduction, and GO:0008219: cell death, were comparable to those for the functional categories other than the immune-related genes. Genes in these three categories have also been reported to have a higher non-synonymous/synonymous substitution ratio than the genes in the other categories (Clark et al. 2003; Gibbs et al. 2007; Nielsen et al. 2005).

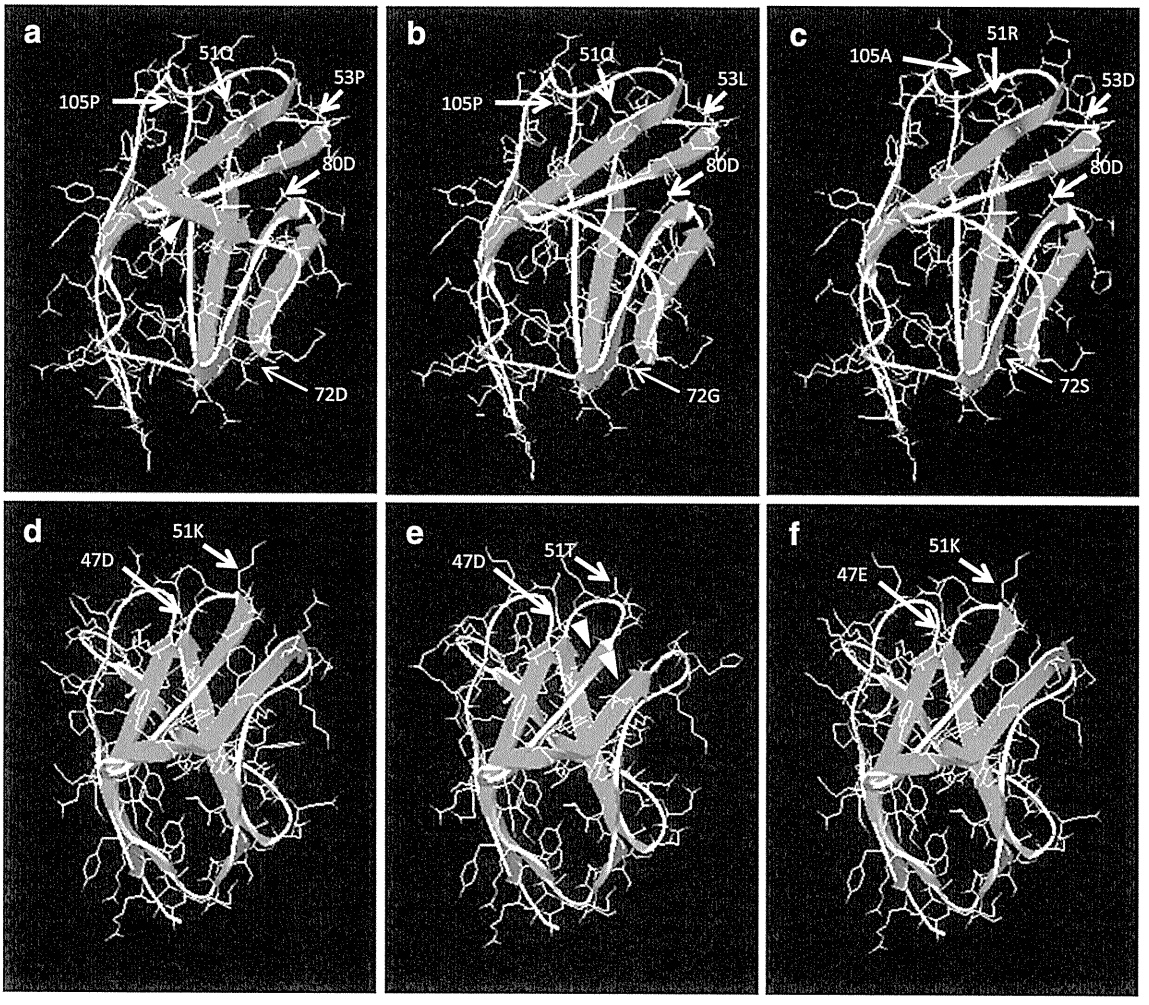

Fig. 5 Three-dimensional structures of CD3E and CD3G modeled by SWISS-MODEL. Arrows indicate amino acid sites identified as being under positive selection by using the BEB method in the PAML program. **a** Human CD3E. An *arrowhead* indicates a β-strand which is unique to human CD3E. **b** rhesus macaque CD3E, **c** marmoset CD3E, **d** human CD3G, **e** rhesus macaque CD3G. *Arrowheads* indicate short strands of β-strand which are unique to rhesus CD3G. **f** marmoset CD3G

It has been reported that the average value of ω in the human lineage is higher than that in the other primate lineages (Ellegren 2008; Gibbs et al. 2007; Kosiol et al. 2008). The differences in the ω among the primate lineages may be attributable to the differences in the effective population size during the course of evolution (Bakewell et al. 2007). Interestingly, in our study, the average value of ω for immune-related genes in the human lineage was the lowest among the primate lineages. Because previous studies suggest that the rapid evolution of the immune-related genes may be due to a direct consequence of complex selection pressure exerted by infectious reagents including microbes and viruses (Barreiro and Quintana-Murci 2010), the observation in our study led us to a hypothesis that in the course of human evolution there might be fewer challenges from pathogens than the other primates, in part due to a shorter course of human evolution. In support of this, it was reported that humans had faced relatively fewer challenges from retroviruses and that humans were consequently at present more susceptible to retrovirus infections than the other primates (Sawyer et al. 2006). However, such a slow evolution of human lineage might also be caused by other factors such as long generation time and small population size.

We identified 11 genes possibly having undergone positive selective pressure (Table 1). Among them, *SIGLEC5*, *CD33*, *CD4*, and *CD3E* have been reported to be genes under the pressure of positive selection in the primate evolution (Angata et al. 2004; Gibbs et al. 2007; Zhang et al. 2008). These genes play crucial roles in the innate and adaptive immune systems, and infectious pathogens might have exerted selective pressure on them (Angata 2006; Crocker et al. 2007), because SIGLEC5, CD33 (SIGLEC3), and CD4 are cell surface receptors for microorganisms.

CD3E and *CD3G* encode the components of T cell antigen receptor (TCR) complex, TCR–CD3 complex. The

TCR–CD3 complex plays a key role in the regulation of immune system through the recognition of antigenic peptides presented by MHC molecules, and mutations in either *CD3E* or *CD3G* are known to cause primary immunodeficiency in humans (Buckley 2004; de Saint et al. 2004; Recio et al. 2007; Sun et al. 2001). Furthermore, previous studies have revealed the role of Ig domains of CD3E and CD3G. For example, cell surface expression of the stable TCR on mature T cell, assembly of the components of T cell antigen receptor complex and T cell activity are regulated by the Ig domains of CD3E and CD3G (Dietrich et al. 1996; Guy and Vignali 2009; Sun et al. 2001).

Because we hypothesized that co-evolution might occur between *CD3E* and *CD3G*, protein coding sequences of these *CD3* genes from 23 primate species were determined, and it was suggested that the Ig domains of both CD3E and CD3G have undergone positive Darwinian selection pressure in the primate evolution, especially in the Old World monkey ancestor lineage. However, the role of Ig domains in the direct interaction of CD3E and CD3G has not been reported. Although the direct demonstration of functional interaction are needed to clarify the impacts of AA substitutions on the function of CD3E and CD3G, we modeled three-dimensional structures of the Ig domains of CD3E using SWISS-MODEL, an Automated Comparative Protein Modeling Server (http://swissmodel.expasy.org/SWISS-MODEL.html; Bordoli et al. 2009). As shown in Fig. 5, eight, seven, and seven β-strands were found in the Ig domains of CD3E from human, rhesus macaque, and common marmoset, respectively, and the three AA insertion/deletion observed in the Ig domain appeared to have a strong impact on the modeled structure. In addition, it was possible that five AA sites in the Ig domain, which were identified as target sites for the positive selection, would change the Ig domain structure. It has been reported that highly conserved CXXCXEXXX motifs in the CD3 family play an important role in the molecular interactions among components of the TCR–CD3 complex (Borroto et al. 1998; Xu et al. 2006). Because the Ig domains are localized just upstream of the N-terminal of CXXCXEXXX motifs, drastic structural changes in the Ig domains might affect the functional properties of CD3E and CD3G. It is likely that such structural changes would affect the stability of the TCR–CD3 complex and the expression level in mature T cells (Call and Wucherpfennig 2004; Guy and Vignali 2009; Wang et al. 1998).

What was the extent of selective pressure exerted on *CD3E* and *CD3G* in the course of primate evolution? Given that the TCR–CD3 complex plays a crucial role in the regulation of immune system, infectious diseases and autoimmunity have been postulated to be the strongest selective pressures (Robins et al. 2009; Sun et al. 2001). It is widely accepted that the susceptibility to infectious pathogens, such as *Mycobacterium tuberculosis bacilli* and HIV-1, are different among primate species (Lyashchenko et al. 2008; Song et al. 2005). Because the dn values for the Ig domains of *CD3E* and *CD3G* are significantly greater than the ds values in the Old World monkey ancestor lineage, their ancestors might have been exposed to powerful selective pressure. To clarify the selective pressure exerted on *CD3E* and *CD3G*, further study on phenotypic differences, such as the relative susceptibilities to infectious pathogens and/or autoimmune disease, among various primate species is needed.

In conclusion, we investigated the molecular evolution of IgSF genes in primates. The study has demonstrated that the immune-related IgSF genes have high non-synonymous/synonymous substitution rates, and those 11 IgSF genes, namely *SIGLEC5*, *SLAMF6*, *CD33*, *CD3E*, *CEACAM8*, *CD3G*, *FCER1A*, *CD48*, *CD4*, *TIM4*, and *FCGR2A*, may undergo the positive selective pressure in the primate evolution.

Acknowledgments This work was supported in part by research grants from the Ministry of Health, Labor and Welfare, Japan, the Japan Health Science Foundation, the program of Founding Research Centers for Emerging and Reemerging Infection Disease, the program of Research on Publicly Essential Drugs and Medical Devices, by grant-in-aids for Scientific research from the Ministry of Education, Culture, Sports, Science, and Technology (MEXT), Japan, by a grant from the Life Science Institute Foundation, Japan, and by grants for India–Japan Cooperative Science Program from Japan Society for the Promotion of Science (JSPS), Japan and Department of Science and Technology (DST), India.

References

Angata T, Margulies EH, Green ED, Varki A (2004) Large-scale sequencing of the CD33-related Siglec gene cluster in five mammalian species reveals rapid evolution by multiple mechanisms. Proc Natl Acad Sci USA 101:13251–6

Angata T (2006) Molecular diversity and evolution of the Siglec family of cell-surface lectins. Mol Divers 10:555–66

Ashburner M, Ball CA, Blake JA, Botstein D, Butler H, Cherry JM, Davis AP, Dolinski K, Dwight SS, Eppig JT, Harris MA, Hill DP, Issel-Tarver L, Kasarskis A, Lewis S, Matese JC, Richardson JE, Ringwald M, Rubin GM, Sherlock G (2000) Gene ontology: tool for the unification of biology. The Gene Ontology Consortium. Nat Genet 25:25–9

Bakewell MA, Shi P, Zhang J (2007) More genes underwent positive selection in chimpanzee evolution than in human evolution. Proc Natl Acad Sci USA 104:7489–94

Barclay AN (2003) Membrane proteins with immunoglobulin-like domains—a master superfamily of interaction molecules. Semin Immunol 15:215–23

Barreiro LB, Quintana-Murci L (2010) From evolutionary genetics to human immunology: how selection shapes host defence genes. Nat Rev Genet 11:17–30

Blanchette M, Kent WJ, Riemer C, Elnitski L, Smit AF, Roskin KM, Baertsch R, Rosenbloom K, Clawson H, Green ED, Haussler D, Miller W (2004) Aligning multiple genomic sequences with the threaded blockset aligner. Genome Res 14:708–15

Bordoli L, Kiefer F, Arnold K, Benkert P, Battey J, Schwede T (2009) Protein structure homology modeling using SWISS-MODEL workspace. Nat Protoc 4:1–13

Borroto A, Mallabiabarrena A, Albar JP, Martinez AC, Alarcon B (1998) Characterization of the region involved in CD3 pairwise interactions within the T cell receptor complex. J Biol Chem 273:12807–16

Buckley RH (2004) The multiple causes of human SCID. J Clin Invest 114:1409–11

Call ME, Wucherpfennig KW (2004) Molecular mechanisms for the assembly of the T cell receptor-CD3 complex. Mol Immunol 40:1295–305

Chatterjee HJ, Ho SY, Barnes I, Groves C (2009) Estimating the phylogeny and divergence times of primates using a supermatrix approach. BMC Evol Biol 9:259

Clark AG, Glanowski S, Nielsen R, Thomas PD, Kejariwal A, Todd MA, Tanenbaum DM, Civello D, Lu F, Murphy B, Ferriera S, Wang G, Zheng X, White TJ, Sninsky JJ, Adams MD, Cargill M (2003) Inferring nonneutral evolution from human–chimp–mouse orthologous gene trios. Science 302:1960–3

Consortium CSaA (2005) Initial sequence of the chimpanzee genome and comparison with the human genome. Nature 437:69–87

Crocker PR, Paulson JC, Varki A (2007) Siglecs and their roles in the immune system. Nat Rev Immunol 7:255–66

de Saint BG, Geissmann F, Flori E, Uring-Lambert B, Soudais C, Cavazzana-Calvo M, Durandy A, Jabado N, Fischer A, Le Deist F (2004) Severe combined immunodeficiency caused by deficiency in either the delta or the epsilon subunit of CD3. J Clin Invest 114:1512–7

Dietrich J, Neisig A, Hou X, Wegener AM, Gajhede M, Geisler C (1996) Role of CD3 gamma in T cell receptor assembly. J Cell Biol 132:299–310

Ellegren H (2008) Comparative genomics and the study of evolution by natural selection. Mol Ecol 17:4586–96

Gibbs RA et al (2007) Evolutionary and biomedical insights from the rhesus macaque genome. Science 316:222–34

Goh CS, Bogan AA, Joachimiak M, Walther D, Cohen FE (2000) Co-evolution of proteins with their interaction partners. J Mol Biol 299:283–93

Guy CS, Vignali DA (2009) Organization of proximal signal initiation at the TCR:CD3 complex. Immunol Rev 232:7–21

Halaby DM, Mornon JP (1998) The immunoglobulin superfamily: an insight on its tissular, species, and functional diversity. J Mol Evol 46:389–400

Jothi R, Cherukuri PF, Tasneem A, Przytycka TM (2006) Co-evolutionary analysis of domains in interacting proteins reveals insights into domain–domain interactions mediating protein-protein interactions. J Mol Biol 362:861–75

Kent WJ, Baertsch R, Hinrichs A, Miller W, Haussler D (2003) Evolution's cauldron: duplication, deletion, and rearrangement in the mouse and human genomes. Proc Natl Acad Sci USA 100:11484–9

Kosiol C, Vinar T, da Fonseca RR, Hubisz MJ, Bustamante CD, Nielsen R, Siepel A (2008) Patterns of positive selection in six mammalian genomes. PLoS Genet 4:e1000144

Lander ES et al (2001) Initial sequencing and analysis of the human genome. Nature 409:860–921

Larkin MA, Blackshields G, Brown NP, Chenna R, McGettigan PA, McWilliam H, Valentin F, Wallace IM, Wilm A, Lopez R, Thompson JD, Gibson TJ, Higgins DG (2007) Clustal W and Clustal X version 2.0. Bioinformatics 23:2947–8

Li Y, Wallis M, Zhang YP (2005) Episodic evolution of prolactin receptor gene in mammals: coevolution with its ligand. J Mol Endocrinol 35:411–9

Lyashchenko KP, Greenwald R, Esfandiari J, Chambers MA, Vicente J, Gortazar C, Santos N, Correia-Neves M, Buddle BM, Jackson R, O'Brien DJ, Schmitt S, Palmer MV, Delahay RJ, Waters WR (2008) Animal-side serologic assay for rapid detection of *Mycobacterium bovis* infection in multiple species of free-ranging wildlife. Vet Microbiol 132:283–92

Nei M, Gojobori T (1986) Simple methods for estimating the numbers of synonymous and nonsynonymous nucleotide substitutions. Mol Biol Evol 3:418–26

Nielsen R, Bustamante C, Clark AG, Glanowski S, Sackton TB, Hubisz MJ, Fledel-Alon A, Tanenbaum DM, Civello D, White TJ, Sninsky JJ, Adams MD, Cargill M (2005) A scan for positively selected genes in the genomes of humans and chimpanzees. PLoS Biol 3:e170

Otey CA, Dixon R, Stack C, Goicoechea SM (2009) Cytoplasmic Ig-domain proteins: cytoskeletal regulators with a role in human disease. Cell Motil Cytoskeleton 66:618–34

Recio MJ, Moreno-Pelayo MA, Kilic SS, Guardo AC, Sanal O, Allende LM, Perez-Flores V, Mencia A, Modamio-Hoybjor S, Seoane E, Regueiro JR (2007) Differential biological role of CD3 chains revealed by human immunodeficiencies. J Immunol 178:2556–64

Robins HS, Campregher PV, Srivastava SK, Wacher A, Turtle CJ, Kahsai O, Riddell SR, Warren EH, Carlson CS (2009) Comprehensive assessment of T-cell receptor beta-chain diversity in alphabeta T cells. Blood 114:4099–107

Rzhetsky A, Nei M (1993) Theoretical foundation of the minimum-evolution method of phylogenetic inference. Mol Biol Evol 10:1073–95

Sawyer SL, Wu LI, Akey JM, Emerman M, Malik HS (2006) High-frequency persistence of an impaired allele of the retroviral defense gene TRIM5alpha in humans. Curr Biol 16:95–100

Song B, Javanbakht H, Perron M, Park DH, Stremlau M, Sodroski J (2005) Retrovirus restriction by TRIM5alpha variants from Old World and New World primates. J Virol 79:3930–7

Sun ZJ, Kim KS, Wagner G, Reinherz EL (2001) Mechanisms contributing to T cell receptor signaling and assembly revealed by the solution structure of an ectodomain fragment of the CD3 epsilon gamma heterodimer. Cell 105:913–23

Wang B, Wang N, Salio M, Sharpe A, Allen D, She J, Terhorst C (1998) Essential and partially overlapping role of CD3gamma and CD3delta for development of alphabeta and gammadelta T lymphocytes. J Exp Med 188:1375–80

Wong WS, Yang Z, Goldman N, Nielsen R (2004) Accuracy and power of statistical methods for detecting adaptive evolution in protein coding sequences and for identifying positively selected sites. Genetics 168:1041–51

Xu C, Call ME, Wucherpfennig KW (2006) A membrane-proximal tetracysteine motif contributes to assembly of CD3deltaepsilon and CD3gammaepsilon dimers with the T cell receptor. J Biol Chem 281:36977–84

Yang Z (2005) The power of phylogenetic comparison in revealing protein function. Proc Natl Acad Sci USA 102:3179–80

Yang Z (2007) PAML 4: phylogenetic analysis by maximum likelihood. Mol Biol Evol 24:1586–91

Yang Z, Nielsen R (2000) Estimating synonymous and nonsynonymous substitution rates under realistic evolutionary models. Mol Biol Evol 17:32–43

Yang Z, Wong WS, Nielsen R (2005) Bayes empirical bayes inference of amino acid sites under positive selection. Mol Biol Evol 22:1107–18

Yu XJ, Zheng HK, Wang J, Wang W, Su B (2006) Detecting lineage-specific adaptive evolution of brain-expressed genes in human using rhesus macaque as outgroup. Genomics 88:745–51

Zhang J, Rosenberg HF, Nei M (1998) Positive Darwinian selection after gene duplication in primate ribonuclease genes. Proc Natl Acad Sci USA 95:3708–13

Zhang ZD, Weinstock G, Gerstein M (2008) Rapid evolution by positive Darwinian selection in T-cell antigen CD4 in primates. J Mol Evol 66:446–56